

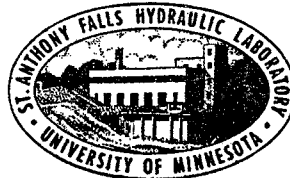
UNIVERSITY OF MINNESOTA
ST. ANTHONY FALLS HYDRAULIC LABORATORY

Technical Paper No. 54, Series B

On the Existence of Zero Form-Drag and Hydrodynamically Stable Supercavitating Hydrofoils

by

R. OBA



Prepared for
OFFICE OF NAVAL RESEARCH
Department of the Navy
Washington, D.C.
under
Contract Nonr 710(24), Task NR 062-052

November 1965
Minneapolis, Minnesota

University of Minnesota
ST. ANTHONY FALLS HYDRAULIC LABORATORY

FINAL REPORT
FLOW STUDIES ABOUT BODIES AT LOW CAVITATION NUMBERS
Contract Nonr 710(24), Task NR 062-052

Prepared for
OFFICE OF NAVAL RESEARCH
Department of the Navy
Washington, D. C.
under
Contract Nonr 710(24), Task NR 062-052

March 1966

Final Report
FLOW STUDIES ABOUT BODIES AT LOW CAVITATION NUMBERS
Contract Nonr 710(24), Task NR 062-052

Historical Summary

This contract became effective on July 1, 1957, replacing an earlier contract in a related area. It has been continuously active until it was finally terminated on July 31, 1965. During this eight-year period the contract supported experimental research conducted in the vertical free-jet water tunnel at the St. Anthony Falls Hydraulic Laboratory and some analytical research as well. From August 1, 1963, to the termination, it also supported some of the experimental research on hydrofoils conducted in the towing tank.

The research began as general research on supercavitating flows when the possible utility of such flows first became apparent. However, the emphasis has been largely on applications to hydrofoils, especially in the later years. This emphasis resulted in a shift of support from ONR funds to BUSHIPS funds and to the final termination of the contract. Some of the research previously conducted under this contract is currently being supported from Laboratory funds and the free-jet tunnel is being used on this research as well as on other contract research.

The technical papers and publications prepared under Contract Nonr 710(24) are listed in the Appendix.

Technical Summary

The first work under this contract dealt with experimental verification of theoretical predictions for shape of cavities and drag and lift for bodies in a free jet. This research led to the design of a two-dimensional test section which fitted within the originally axially-symmetric test section of the free-jet tunnel. The results were published in Project Report No. 59 which appeared in the Journal of Fluid Mechanics.

The early research indicated the limitations of the hybrid test section. This was replaced by an entirely new two-dimensional test section described in Technical Papers No. 24-B and 40-B. The two-dimensional test

section and especially its dynamometers have been modified since, but there have been no major changes in the configuration.

The early research led to an attempt to study supercavitation by injecting air into the wakes of otherwise non-cavitating bodies. Study of such ventilation-produced cavitation was appealing because it would permit parallel studies to be conducted in the free-jet tunnel and in the towing tank at the Laboratory. Both naturally occurring and ventilated cavities could be studied in the new test section of the tunnel whereas only ventilated cavities could be studied in the towing tank. However, three-dimensional bodies of larger size could be used in the tank, and also gravity acted in the right direction. Some results of the towing tank tests (relative to tandem interference effects) are illustrated by Memorandum No. M-92 and Technical Paper No. 50-B.

One of the major discoveries of the research was the occurrence of pulsation in ventilated cavities once the cavitation number decreased beyond a certain minimum determined by the flow conditions. The pulsation research is reported in Technical Papers No. 29-B and 32-B which have appeared in the Journal of Ship Research and in the Proceedings of the Fourth Symposium on Naval Hydrodynamics.

During the ventilation research it was observed that ventilation had a material effect on noise reduction due to cavitation. Some noise research was conducted in the tunnel as reported in Technical Paper No. 33-B. In general, the tunnel has too high a background noise level to be useful for all but the most intense noises.

The research, which was originally concerned with essentially mean steady flows, gradually shifted to unsteady flows associated with waves on free surfaces, with acceleration and deceleration of bodies, and with the operation of flaps. The experimental research was preceded by and accompanied by analytical research described in Technical Papers No. 34-B, 38-B, 39-B, and 43-B in this area. Experimental results for unsteady flows associated with a supercavitating plate oscillating at low frequencies are reported in Technical Paper No. 49-B. Unsteady flows due to small amplitude and high frequency oscillation of a solid flap attached to a supercavitating plate were studied experimentally and theoretically and the results are described in Technical Paper No. 52-B.

One of the apparent problems when flaps are used with supercavitating hydrofoils was the possibility that leakage through the flap hinge would have a deleterious effect on performance. This problem was analyzed in Technical Paper No. 51-B and, from another more general viewpoint, in an as yet unpublished paper with the predicted result that leakage is probably not an important practical problem.

Recent analytical work on the steady flow, supercavitating problem has involved development of two-dimensional hydrofoil shapes whose lift increases as the foil submerges further below the free surface--the so-called stable hydrofoil. This research is described in Technical Paper No. 54-B, but there has been no time to verify the analytical results experimentally under the contract.

Recent experimental research has involved hydrofoils with oscillating flaps at non-zero cavitation numbers produced largely by ventilation at reduced frequencies up to about four. However, analysis which has proceeded subsequent to termination of the contract is not completed and there are some gaps in the experimental data. It is intended to submit an article for publication in a periodical when the analysis is completed. Some preliminary conclusions are:

1. Flap oscillation causes cavity pressure of a ventilated cavity to oscillate along with lift, drag, and moment. Lift coefficient oscillation is larger than at zero cavitation number and first increases and then decreases as the reduced frequency is increased. This trend is opposite to the zero cavitation number case.
2. If the flap is operated at a frequency near or above the natural frequency of a ventilated cavity, the cavity may become unstable and change its regime to that of a longer or shorter cavity. There may also be a step change in the oscillating force and moment coefficients.
3. In general, cavity oscillations due to pulsation associated with ventilation and due to operation of a flap add linearity. However, at frequencies near the natural cavity frequency, they have also been observed to cancel, leaving a non-pulsating cavity.

This summary report of Contract Nonr 710(24) is being transmitted to all those on the distribution lists for Technical Papers 52-B and 54-B.

APPENDIX

Reports and Publications Prepared under Contract 710(24)

- Project Report No. 59, Experimental Studies of Supercavitating Flow about Simple Two-Dimensional Bodies in a Jet, by Edward Silberman, 1958 (also in Journal of Fluid Mechanics, Vol. 5, Part 3, 1959).
- Technical Paper No. 24-B, The St. Anthony Falls Hydraulic Laboratory Gravity-Flow Free-Jet Water Tunnel, by Edward Silberman and John F. Ripken, 1959.
- Technical Paper No. 29-B, Instability of Ventilated Cavities, by Edward Silberman and C. S. Song, 1959 (also in Journal of Ship Research, Vol. 5, No. 1, June 1961).
- Technical Paper No. 32-B, Pulsation of Ventilated Cavities, by C. S. Song, 1960 (also in Journal of Ship Research, Vol. 5, No. 4, March 1962).
- Technical Paper No. 33-B, Experimental Studies of Cavitation Noise in a Free-Jet Tunnel, by C. S. Song, 1961.
- Technical Paper No. 34-B, Unsteady, Symmetrical, Supercavitating Flows Past a Thin Wedge in a Jet, by C. S. Song, 1962.
- Technical Paper No. 38-B, Unsteady, Symmetrical, Supercavitating Flows Past a Thin Wedge in a Solid Wall Channel, by C. S. Song and F. Y. Tsai, 1962.
- Pulsation of Two-Dimensional Cavities, by C. S. Song, Fourth Symposium on Naval Hydrodynamics, Office of Naval Research, August 1962.
- Technical Paper No. 39-B, A Note on the Linear Theory of Two-Dimensional Separated Flows about Thin Bodies, by C. S. Song, 1962.
- Technical Paper No. 40-B, A Dynamometer for the Two-Dimensional, Free-Jet Water Tunnel Test Section, by Edward Silberman and R. H. Daugherty, 1962.
- Technical Paper No. 43-B, A Quasi-Linear and Linear Theory for Non-Separated and Separated Two-Dimensional, Incompressible, Irrotational Flow about Lifting Bodies, by C. S. Song, 1963.
- Memorandum No. M-92, Interference Effects for Tandem Fully Submerged Flat Noncavitating Hydrofoils, by W. H. C. Maxwell, 1963.
- Technical Paper No. 49-B, Measurements of the Unsteady Force on Cavitating Hydrofoils in a Free Jet, by C. S. Song, 1964.
- Technical Paper No. 50-B, Tandem Interference Effects for Noncavitating and Supercavitating Hydrofoils, by J. M. Wetzell, 1965.
- Technical Paper No. 51-B, Performance of Supercavitating Hydrofoils with Flaps, with Special Reference to Leakage and Optimization of Flap Design, by R. Oba, 1965.
- Technical Paper No. 52-B, Supercavitating Flat-Plate with an Oscillating Flap at Zero Cavitation Number, by C. S. Song, 1965.
- Technical Paper No. 54-B, On the Existence of Zero Form-Drag and Hydrodynamically Stable Supercavitating Hydrofoils, by R. Oba, 1965.

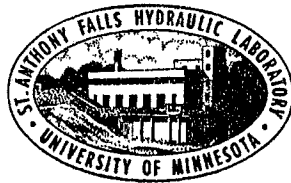
UNIVERSITY OF MINNESOTA
ST. ANTHONY FALLS HYDRAULIC LABORATORY

Technical Paper No. 54, Series B

On the Existence of Zero Form-Drag and Hydrodynamically Stable Supercavitating Hydrofoils

by

R. OBA



Prepared for
OFFICE OF NAVAL RESEARCH
Department of the Navy
Washington, D.C.
under
Contract Nonr 710(24), Task NR 062-052

November 1965
Minneapolis, Minnesota

Reproduction in whole or in part is permitted
for any purpose of the United States Government

ABSTRACT

The linearized complex acceleration potential is obtained for a hydrofoil of arbitrary shape in steady motion beneath a free surface with cavity of infinite length in simple and compact form. Under appropriate limiting conditions, it is shown that the solutions obtained from this potential reduce to the known solutions of Green for a planing foil, and of Auslaender and Hsu for a flat plate foil with or without flat flap near the free surface.

Using some numerical results obtained from the complex potential, it is shown that there exists theoretically a supercavitating hydrofoil with finite lift coefficient and zero form drag. It is also shown that there exists theoretically a supercavitating hydrofoil with stable characteristics when shallowly submerged; that is, the lift coefficient increases as the submergence increases. Possible shapes for these hydrofoils are suggested so that the free streamlines from the leading edges do not intersect the foil surface (the hydrofoils are physically real) and so that the pressure on the pressure surface is everywhere greater than cavity pressure and less than stagnation pressure (except near the leading and trailing edges).

CONTENTS

	Page
Abstract	iii
List of Illustrations	vii
List of Tables	ix
List of Symbols	xi
I. INTRODUCTION	1
II. BASIC EQUATIONS	2
III. LIFT, DRAG, AND MOMENT	8
IV. RESTRICTIONS FOR THE FOIL SHAPE PARAMETERS A_n	14
A. Case of Shallow Submergence	15
B. Case of Deeper Submergence	17
V. EXISTENCE OF ZERO FORM-DRAG HYDROFOILS	17
VI. THE EXISTENCE OF HYDRODYNAMICALLY STABLE HYDROFOILS OPERATING NEAR A FREE SURFACE	21
VII. CONCLUSIONS	24
Acknowledgments	26
List of References	27
Figures 1 through 16	31
Appendix	45

LIST OF ILLUSTRATIONS

Figure		Page
1	Physical Plane, $z = x + iy$	31
2	Mapping Plane by Riegels' Transformation, $\bar{z} = \bar{x} + i\bar{y}$	31
3	Mapping Plane (Lower Half Plane), $\zeta = \xi + i\eta$	31
4	Accuracy of Simple Approximation for y_f for Flat Plate; $A_0 \neq 0, A_1 = A_2 = \dots = 0$	32
5	Change in Spray Angle τ_n due to Submergence H^* for Various Shape Parameters A_n	32
6	Zero Form-Drag Supercavitating Hydrofoil No. 1 at $H^* \approx 0$; $C_L \approx \frac{\pi}{2} A_1, C_D \approx 0, (A_1 \neq 0, A_{n \neq 1} = 0)$	33
7	Zero Form-Drag Supercavitating Hydrofoil No. 2 at $H^* \approx 0$; $C_L \approx \frac{\pi}{2} A_1, C_D \approx 0, (A_1 \neq 0, A_2 \neq 0, A_{n \neq 1,2} = 0)$	33
8	Performance of A_1 -Hydrofoil at Deeper Submergence	34
9	Performance of SH1 and SH2 Hydrofoils as a Function of Submergence H^*	35
10	Hydrofoil Shapes and Suction-Side Free Streamline Shapes y_f for Various Submergences H^* of SH1 and SH2 Hydrofoils	36
11	Surface Velocity Distribution u_s for Various Submergences H^* of SH1 and SH2 Hydrofoils	37
12	Performance of the \bar{A}_1 Approximate Circular Arc Hydrofoil	38
13	Surface Velocity Distribution u_s of the Flat Plate Hydrofoil	39
14	Performances of the \bar{A}_2 , S-Cambered Hydrofoil	40
15	Relationship between Cavity Thickness T and the Change in Lift Coefficient as Related to Submergences H^* for the Flat Plate	41
16	Comparison between the Calculated Spray Thickness δ and the Experimental One by Johnson	41

LIST OF TABLES

Table		Page
1	Auxiliary Parameter a	6
2	x_s as a Function of ξ_s for the Foil Pressure Side	6
3	Auxiliary Lift Parameters M_n	12
4	Auxiliary Drag Parameters N_n	12
5	Auxiliary Moment Parameters O_n	13
6	Auxiliary Free Streamline Shape Parameters y_{fA_n} . .	18

LIST OF SYMBOLS

- $\vec{a} = a_x - ia_y$ - flow acceleration
- A, a, a_1 - auxiliary parameters related only to H^*
- A_n ($n = 0, 1, \dots$) - hydrofoil shape parameters
- B_n ($n = 0, 1, \dots$) - auxiliary hydrofoil shape parameters
- C_D - drag coefficient
- C_L - lift coefficient
- C_M - moment coefficient
- $\vec{F} = \phi + i\psi$ - complex acceleration potential
- H - actual submergence
- H^* - modified submergence
- I_n ($n = 0, 1, \dots$) - cavity functions
- J - correction factor for second order terms to increase the accuracy of linearized solutions
- M_n ($n = 0, 1, \dots$) - auxiliary lift parameters
- N_n ($n = 0, 1, \dots$) - auxiliary drag parameters
- O_n ($n = 0, 1, \dots$) - auxiliary moment parameters
- p - perturbation static pressure due to presence of the hydrofoil
- $\vec{q} = 1 + u - iv$ - normalized flow velocity taking the uniform flow velocity as unity
- $\vec{V} = u - iv$ - perturbation velocity due to presence of the hydrofoil
- y_{fA_n} ($n = 0, 1, \dots$) - auxiliary free streamline shape parameters
- $z = x + iy$ - physical plane
- $\bar{z} = \bar{x} + i\bar{y}$ - Riegels' mapping plane
- δ - spray thickness
- $\zeta = \xi + i\eta$ - mapping plane
- ρ - fluid density

τ - spray angle

$v = 2\zeta - 1$ - parameter

Subscripts

f - on the suction-side free streamline

s - on the boundary (real axis of \bar{z} - and ζ -planes)

T - at the trailing edge

x - in the free stream direction

y - normal to the free stream direction

max - maximum

All velocities are normalized with the free stream velocity and all lengths with the chord length.

ON THE EXISTENCE OF
ZERO FORM-DRAG AND HYDRODYNAMICALLY STABLE
SUPERCAVITATING HYDROFOILS

I. INTRODUCTION

Increasing interest in supercavitating hydrofoils has pointed to the need for more precise and more detailed information on the characteristics of such foils operating near a free surface, and to the need for developing better foil performance.

According to the literature, Green [1]¹, in a pioneer work, analyzed performance of the supercavitating flat plate hydrofoil, a very special hydrofoil of exceptionally high drag. Recently, Auslaender [2] analyzed the performance of the supercavitating flapped hydrofoil composed of a flat foil and a flat flap. Auslaender [3] and Luu and Fruman [4] proposed a method to calculate the hydrofoil shape for a given surface pressure distribution (inverse method), and Johnson [5] proposed a very simple approximate method to obtain foil performance (direct method) in which the effects of the free surface are very roughly approximated by a single vortex in the mapping plane. In addition to these works, several experimental studies have also been published.

At this stage, however, the performance of presently available supercavitating hydrofoils operating near a free surface is not necessarily good enough to apply to a practical high-speed surface craft and there remain some basic difficulties. The first difficulty concerns the hydrodynamic stability of the hydrofoil. Most of the known supercavitating hydrofoils are unstable when operated under a free surface; that is, the lift decreases as the submergence becomes greater. Consequently, a supercavitating hydrofoil boat may be unstable in rolling, pitching, and heaving motions. Two well-known methods of providing stability are (1) to use dihedral foils, and (2) to use control devices. The first method will result inevitably in higher drag and lower efficiency. The second method introduces an additional technical problem, the unsteady characteristics of the control devices themselves.

The second basic difficulty is that the efficiency (lift-drag ratio) of supercavitating hydrofoils is, in general, not as high as that of fully

¹Numbers in brackets refer to the List of References on page 27.

wetted hydrofoils and airfoils. A third difficulty arises in that the unsteady characteristics of low drag cambered hydrofoils cannot be predicted.

In this report, possibilities for removing the first and second difficulties given will be discussed theoretically. First, by improving Johnson's approximate method [5], an accurate method to estimate the performance of supercavitating hydrofoils of quite arbitrary shape¹ operating at quite arbitrary submergence is proposed. After rather complicated numerical computations it will be shown that a hydrodynamically stable supercavitating hydrofoil exists for which lift increases with submergence for small submergence. The theory also indicates the existence of an infinite number of zero form-drag hydrofoils with finite lift satisfying the necessary and sufficient conditions for the supercavitating flow of positive cavity thickness and positive surface pressure on the pressure side.

II. BASIC EQUATIONS

The two-dimensional, incompressible, inviscid flow around a supercavitating hydrofoil of arbitrary shape $y_s(x)$ operating near a free surface, in the physical plane $z = x + iy$, is shown in Fig. 1. To simplify the present problem, it is assumed that the foil chord is unity, the leading edge is located on the origin of the coordinate system, and the uniform flow velocity, taken as unity, is the normalizing velocity for all velocities. These assumptions do not limit the scope of the present problem. In this paper discussion will be limited to the special infinite trailing cavity case; also infinite Froude number is assumed.

The flow velocity \vec{q} at any point may be expressed as the sum of the uniform velocity of unit magnitude and the perturbation velocity due to presence of the hydrofoil $u(x, y) - iv(x, y)$, as follows:

$$\vec{q} = 1 + u(x, y) - iv(x, y) = 1 + \vec{V} \quad (1)$$

Assuming that $u, v \ll 1$ and neglecting second order terms, the Eulerian equation of motion may be expressed as

¹As shown later, the hydrodynamically stable hydrofoils have larger camber near their trailing edges. For such hydrofoils, it is doubtful that Johnson's approximate solution [5] would apply.

$$\left(\frac{\partial}{\partial t} + \frac{\partial}{\partial x}\right) \vec{q} = -\frac{1}{\rho} \text{grad } p = \text{grad } \phi \quad (2)$$

where $\phi(x, y, t) = -\frac{p}{\rho}$, ρ is the constant fluid density, p is the perturbation pressure due to the presence of the hydrofoil, and ϕ is the Prandtl acceleration potential.

The equation of continuity and the assumption of $u, v \ll 1$ lead to the following result for the acceleration $\vec{a} = a_x - ia_y$:

$$\text{div } \vec{a} = 0 \quad (3)$$

Then the acceleration potential ϕ satisfies the Laplace equation,

$$\nabla^2 \phi = 0 \quad (4)$$

Therefore, a conjugate function ψ and a complex acceleration potential $\vec{F}(x, y, t)$ may be defined as follows:

$$\frac{\partial \phi}{\partial x} = \frac{\partial \psi}{\partial y} = a_x, \quad \frac{\partial \phi}{\partial y} = -\frac{\partial \psi}{\partial x} = a_y \quad (5)$$

$$\vec{F}(x, y, t) = \phi + i\psi \quad (6)$$

Then

$$\frac{d\vec{F}}{dz} = \vec{a} = a_x - ia_y = \left(\frac{\partial}{\partial t} + \frac{\partial}{\partial x}\right) \vec{V} \quad (7)$$

For the steady case

$$\frac{d\vec{F}}{dz} = \frac{d\vec{V}}{dz}, \quad \phi + i\psi = u - iv \quad (8)$$

Next, boundary conditions are considered. By Riegels' transformation [6] the present rather complicated boundary value problem shown in Fig. 1 can be reduced to a rather simple boundary value problem on the \bar{z} -plane, shown in Fig. 2, in which the boundary values are given only on straight slits \overline{CD} , \overline{OD} , and \overline{OB} . Here, the following relation holds between the boundary values in the z -plane and those in the \bar{z} -plane:

$$1 + \vec{F}_s(z) = \frac{1 + \vec{F}_s(\bar{z})}{\sqrt{1 + \left(\frac{dy}{dx}\right)_s^2}} \quad (9)$$

where the subscript s means "on the boundary" and $x_s = \bar{x}_s$. $\left(\frac{dy}{dx}\right)_s$ is the slope of the boundary line. If $u_s, v_s, \left(\frac{dy}{dx}\right)_s \ll 1$,

$$\vec{F}_s(z) = \vec{F}_s(\bar{z}) + O(\epsilon^2) \quad (10)$$

The modified submergence H^* in the mapping plane \bar{z} , shown in Fig. 2, has still not been determined. H^* is not necessarily equal to the actual submergence H , since H does not indicate the mean free surface level, especially for the flat plate hydrofoil¹ at small submergence with a rather large spray angle (see Fig. 5). However, since low drag, cambered hydrofoils generally have rather small spray angles, the assumption $H^* \cong H$ might be roughly applied to such cambered hydrofoils.

Finally, the boundary conditions under the assumption of small perturbation may be summarized as follows:

1. Assuming that the disturbance pressure p due to presence of the hydrofoil is zero on the free surfaces, it follows that

$$\phi_s(x) = \phi_s(\bar{x}) = 0 \quad \text{for} \quad \begin{array}{l} \bar{x}_s \geq 0, \quad \bar{y}_s = 0^+ \\ \bar{x}_s \geq 1, \quad \bar{y}_s = 0^- \\ -\infty < \bar{x}_s < \infty, \quad \bar{y}_s = H^{*-} \end{array} \quad (11)$$

2. On the foil surface $y_s(x)$, the linearized boundary condition is

$$\left(\frac{dy}{dx}\right)_s = \frac{v_s}{1 + u_s} = -\psi_s(\bar{x}) + O(\epsilon^2) \quad (12)$$

3. The condition at upstream infinity $z = \bar{z} = -\infty$ is

¹In the Appendix the useful result $H^* \cong \delta$, where δ is the spray thickness (see Fig. 1), was found even for the extreme flat plate case. Also in the Appendix the relation between δ and the submergence H is given.

$$\vec{F}(-\infty) = 0 \quad (13)$$

4. The Kutta Joukowski condition is to be enforced.

Then $\vec{F}(\bar{z})$ is continuous at $\bar{z} = \bar{z}_T$.

These basic equations or boundary conditions may be readily generalized to the unsteady problem for hydrofoils operating near the free surface, that is, the third problem mentioned in the Introduction. This problem will be discussed in a succeeding report. The above boundary conditions are quite similar to the ones given by Johnson [5] if the assumption $H = H^*$ can be accepted.

Now that the boundary conditions have been applied to the mapping plane \bar{z} , the problem solving can begin. First, the \bar{z} -plane is transformed into the lower half ζ -plane by the mapping function [5],

$$\bar{z} = A[\zeta - a \log(1 + \frac{\zeta}{a})] \quad (14)$$

Here auxiliary parameters A and a have been introduced; these are related to the modified submergence H^* as follows:

$$H^* = \pi a A, \quad \frac{1}{A} = 1 - a \ln(1 + \frac{1}{a}) \quad (15)$$

The problem has now been reduced to a very simple boundary value problem in which all boundary values are given only on the real ξ -axis.

Equations (9) and (14) result in

$$x_s = \bar{x}_s = A[\xi_s - a \ln(1 + \frac{\xi_s}{a})] \quad (14')$$

Some numerical data for a vs H^* and x_s vs ξ_s are presented in Tables 1 and 2. More such data can be found in Ref. [7].

Since the complex acceleration potential $\vec{F}(z)$ must satisfy the linear Laplace equation, the general solution may be easily obtained by superposing partial solutions and may be expressed as follows [8][9]:

$$\vec{F}(z) = \vec{F}(\bar{z}) = \vec{F}(\zeta) = i \sum_{n=0}^{\infty} A_n I_n \quad (16)$$

where the A_n are defined in Eq. (19) below and

$$\left. \begin{aligned} I_0 &= 1 - \sqrt{\frac{v-1}{v+1}}, & I_1 &= v - \sqrt{v^2 - 1}, & I_2 &= 1 - 2v I_1; \\ I_{n+1} &= -2v I_n - I_{n-1}; & n &\geq 2; \end{aligned} \right\} \quad (17)$$

$$v = 2\zeta - 1 \quad (18)$$

and where I_0 and I_n are the Hilbert transform of $\cot \frac{\theta}{2}$ and $\sin n\theta$ shown in Eq. (16'') below. On the free surface or on the cavity boundary $|v| \geq 1$ and I_n is real. Then

$$\vec{F}_s(\xi_s) = i\psi_s(\xi_s), \quad \phi_s(\xi_s) = 0 \quad (16')$$

On the foil surface, $-1 \leq v \leq 1$. Then

$$\begin{aligned} \vec{F}_s(x_s) &= \vec{F}_s(\bar{x}_s) = \vec{F}_s(\xi_s) = A_0 \cot \frac{\theta}{2} + \sum_1^{\infty} A_n \sin n\theta - i(-A_0 + \sum_1^{\infty} A_n \cos n\theta) \\ \xi_s &= \frac{1}{2}(1 - \cos \theta), \quad 0 \geq \theta \geq -\pi \end{aligned} \quad (16'')$$

$\vec{F}_s(-\infty) = 0$, and $\vec{F}(\zeta)$ is continuous at $v = 1$ (at the trailing edge where $z_s = 1$). Therefore, the solution $\vec{F}(\zeta)$ satisfies boundary conditions 1, 3, and 4 listed above.

On the physical plane z the hydrofoil shape $y_s(x)$ is given. The foil slope $\left(\frac{dy}{dx}\right)_s$ and then $\psi_s(x_s)$ and $\psi_s(\xi_s)$ are known. Thus the arbitrary constants A_0, A_1, A_2, \dots , which are connected only with the foil shape and the submergence, are determined easily as follows:

$$\left. \begin{aligned} -A_0 &= \frac{1}{\pi} \int_0^{-\pi} \psi_s(\xi) d\theta; \\ A_n &= \frac{2}{\pi} \int_0^{-\pi} \psi_s(\xi) \cos n\theta d\theta, \quad n = 1, 2, 3, \dots \end{aligned} \right\} \quad (19)$$

A flat plate foil is given by $A_0 \neq 0$ and $A_{n \neq 0} = 0$. The greater the number n of A_n , the more cambered is the foil near the leading and/or the trailing edge.

III. LIFT, DRAG, AND MOMENT

The lift, drag, and moment per unit span of foil, respectively, may be expressed in coefficient form as follows:

$$C_L = -\frac{2}{J} \int_0^1 \phi_s(x) dx_s \quad (20)$$

$$C_D = -\frac{2}{J} \int_0^1 \left(\frac{dy}{dx}\right)_s \phi_s(x) dx_s \quad (21)$$

$$C_M = -\frac{2}{J^2} \int_0^1 x_s \phi_s(x) dx_s \quad (22)$$

where J is a correction factor to offset the second order errors due principally to the assumption that the Riegels' factor $\frac{1}{\sqrt{1 + \left(\frac{dy}{dx}\right)_s^2}}$ in Eq. (9)

is unity. From the studies of the arbitrary hydrofoil in infinite fluid [10] and of the flat plate hydrofoil at arbitrary submergence (see the Appendix), the values of J may be expressed approximately as follows:

$$J = \frac{1 + \frac{C_L}{2}}{\cos A_0} + O(\epsilon^2) \quad (23)$$

The lift coefficient C_L is

$$\begin{aligned}
C_L &= -\frac{A}{J} \int_0^{-\pi} \left(A_0 \cot \frac{\theta}{2} + \sum_1^{\infty} A_n \sin n\theta \right) \frac{(1 - \cos\theta) \sin\theta}{1 + 2a - \cos\theta} d\theta \\
&= \frac{\pi A}{2J} \left[2a_1 A_0 + (1 - 4aa_1) A_1 - 4a \sum_2^{\infty} a_1^n A_n \right] \\
&= \frac{1}{J} \sum_0^{\infty} M_n A_n \tag{20'}
\end{aligned}$$

where

$$M_0 = \pi A a_1, \quad M_1 = \frac{\pi A}{2} (1 - 4aa_1);$$

$$M_n = -2\pi A a a_1^n, \quad n \geq 2$$

and

$$a_1 = 1 + 2a - 2a \sqrt{1 + \frac{1}{a}} \tag{24}$$

The drag coefficient C_D is

$$\begin{aligned}
C_D &= \frac{A}{J} \int_0^{-\pi} \left(A_0 \cot \frac{\theta}{2} + \sum_1^{\infty} A_n \sin n\theta \right) \left(-A_0 + \sum_1^{\infty} A_n \cos n\theta \right) \frac{(1 - \cos\theta) \sin\theta}{1 + 2a - \cos\theta} d\theta \\
&= -\frac{\pi A}{2J} \left[\left\{ -2a_1 A_0 + a_1^2 A_1 + (1 - a_1^2) \sum_2^{\infty} a_1^{n-1} A_n \right\} A_0 + \left\{ (1 - 4aa_1) B_1 - 4a \sum_2^{\infty} a_1^n B_n \right\} \right] \\
&= \frac{1}{J} \left(\sum_0^{\infty} N_n A_n A_0 - \sum_1^{\infty} M_n B_n \right) \tag{21'}
\end{aligned}$$

where

$$\begin{aligned}
N_0 &= \pi A a_1, & N_1 &= -\frac{\pi A}{2} a_1^2; & N_n &= -\frac{\pi A}{2} (1 - a_1^2) a_1^{n-1}, & n &\geq 2 \\
B_1 &= -A_0 A_1 & B_5 &= -A_0 A_5 + A_1 A_4 + A_2 A_3 \\
B_2 &= -A_0 A_2 + \frac{1}{2} A_1^2 & B_6 &= -A_0 A_6 + A_1 A_5 + A_2 A_4 + \frac{1}{2} A_3^2 \\
B_3 &= -A_0 A_3 + A_1 A_2 & B_7 &= -A_0 A_7 + A_1 A_6 + A_2 A_5 + A_3 A_4 \\
B_4 &= -A_0 A_4 + A_1 A_3 + \frac{1}{2} A_2^2 & & \dots & & & &
\end{aligned} \quad (25)$$

The moment coefficient C_M is

$$\begin{aligned}
C_M &= -\frac{A_0^2 a}{J^2} \int_0^{-\pi} \left\{ \frac{1 - \cos \theta}{2a} - \ln \left(\frac{1 - \cos \theta}{2a} + 1 \right) \right\} \left(A_0 \cot \frac{\theta}{2} + \sum_1^{\infty} A_n \sin n\theta \right) \frac{(1 - \cos \theta) \sin \theta}{1 + 2a - \cos \theta} d\theta \\
&= \frac{\pi a A^2}{J^2} \left\{ \frac{1}{4a} (1 - 4aa_1) + a_1 \ln 4aa_1 + \sum_{\lambda=1}^{\infty} \frac{a_1^{2\lambda+1}}{\lambda(\lambda+1)} \right\} A_0 \\
&+ \frac{\pi A_0^2 a}{2J^2} \left[\left(\frac{1}{2a} + \ln 4aa_1 \right) A_1 - \frac{A_2}{4a} - 2(1 + 2a \ln 4aa_1) \left(\sum_{n=1}^{\infty} a_1^n A_n \right) \right. \\
&+ \sum_{n=1}^{\infty} \frac{n a_1^{n+1}}{n+1} A_n + \sum_{n=2}^{\infty} \frac{n a_1^{n-1}}{n-1} A_n - 8a \sum_{n=2,4,\dots}^{\infty} \frac{a_1^n}{n} A_n \\
&\left. - 4a \sum_{n=1}^{\infty} \sum_{\lambda=1}^n \frac{n a_1^{2\lambda+n}}{\lambda(\lambda+n)} A_n - 2a \sum_{\substack{n=3 \\ n \neq 2\lambda}}^{\infty} \sum_{\lambda=1}^{n-1} \frac{n a_1^n}{\lambda(n-\lambda)} A_n \right] \\
&\equiv \frac{1}{J^2} \sum_0^{\infty} O_n A_n \quad (22')
\end{aligned}$$

where

$$O_0 = \pi a A^2 \left\{ \frac{a_1}{2a} \left(1 - \frac{a_1}{2} \right) + a_1 \ln 4aa_1 + \sum_{\lambda=1}^{\infty} \frac{a_1^{2\lambda+1}}{\lambda(\lambda+1)} \right\}$$

$$O_1 = \frac{\pi a A^2}{2} \left\{ \left(\frac{1}{2a} + \ln 4aa_1 \right) - T^* a_1 + \frac{a_1^2}{2} - 2aa_1^3 \right\}$$

$$O_2 = \frac{\pi a A^2}{2} \left\{ -\frac{1}{4a} - T^* a_1^2 + \frac{2}{3} a_1^3 + 2a_1 - 4aa_1^2 - 8a \left(\frac{a_1^4}{3} + \frac{a_1^6}{8} \right) \right\}$$

$$O_n = \frac{\pi a A^2}{2} \left\{ -T^* a_1^n + \frac{na_1^{n+1}}{n+1} + \frac{na_1^{n-1}}{n-1} - \frac{8aa_1^n}{n} - \sum_{\lambda=1}^n \frac{4ana_1^{2\lambda+n}}{\lambda(\lambda+n)} - \sum_{\substack{\lambda=1 \\ n \neq 2\lambda}}^{n-1} \frac{2ana_1^n}{\lambda(n-\lambda)} \right\}$$

$$O_n = \frac{\pi a A^2}{a} \left\{ -T^* a_1^n + \frac{na_1^{n+1}}{n+1} + \frac{na_1^{n-1}}{n-1} - \sum_{\lambda=1}^n \frac{4ana_1^{2\lambda+n}}{x(\lambda+n)} - \sum_{\lambda=1}^{n-1} \frac{2ana^n}{\lambda(n-\lambda)} \right\}$$

for even $n \geq 4$
for odd $n \geq 3$

$$T^* = 2 + 4a \ln 4aa_1$$

The coefficients M_n , N_n , and O_n introduced in Eqs. (20'), (21'), and (22') are independent of the hydrofoil shape; these have been calculated and are shown in Tables 3, 4, and 5. These tables show reasonably good convergence in the series for M_n , N_n , and O_n . The series A_n is generally a good convergent series because the hydrofoil form is usually very smooth. Therefore, though the numerical estimations in Eqs. (20'), (21'), and (22') seem at first to be very complicated ones, they may be evaluated readily in the practical case.

For a special limiting case of $H^* \rightarrow \infty$, that is, $H \rightarrow \infty$,

$$C_L = \frac{\pi}{2J} \left(A_0 + A_1 - \frac{A_2}{2} \right) \quad (26)$$

$$C_D = \frac{\pi}{2J} \left(A_0 + \frac{A_1}{2} \right)^2 \quad (27)$$

$$C_M = \frac{\pi}{32J^2} \left(5A_0 + 7A_1 - 7A_2 + 3A_3 - \frac{A_4}{2} \right) \quad (28)$$

TABLE 3

Auxiliary Lift Parameters M_n

H^*	M_0	M_1	M_2	M_3	M_4	M_5	M_6	M_7	M_8	M_9
0	3.1416	1.5708	0	0	0	0	0	0	0	0
0.25	2.3179	1.6184	-0.1821	-0.1099	-0.0664	-0.0400	-0.0242	0	0	0
0.50	2.1808	1.6238	-0.2609	-0.1333	-0.0681	-0.0348	-0.0178	-0.0146	-0.0088	-0.0053
0.75	2.1048	1.6251	-0.3117	-0.1421	-0.0648	-0.0295	-0.0135	-0.0091	-0.0046	-0.0024
1	2.0537	1.6251	-0.3485	-0.1455	-0.0607	-0.0254	-0.0106	-0.0061	-0.0028	-0.0013
2	1.9429	1.6222	-0.4359	-0.1439	-0.0475	-0.0157	-0.0052	-0.0044	-0.0018	-0.0008
5	1.8256	1.6138	-0.5384	-0.1249	-0.0290	-0.0157	-0.0052	-0.0017	-0.0005	-0.0002
10	1.7585	1.6062	-0.6009	-0.1042	-0.0181	-0.0067	-0.0016	-0.0004	-0.0001	0
100	1.6343	1.5858	-0.7218	-0.0432	-0.0026	-0.0031	-0.0005	-0.0001	0	0
∞	1.5708	1.5708	-0.7854	0	0	0	0	0	0	0

TABLE 4

Auxiliary Drag Parameters N_n

H^*	N_0	N_1	N_2	N_3	N_4	N_5	N_6	N_7	N_8	N_9
0	3.1416	-1.5708	0	0	0	0	0	0	0	0
0.25	2.3179	-0.6995	-0.7368	-0.4447	-0.2684	-0.1620	-0.0978	-0.0590	-0.0356	-0.0215
0.50	2.1808	-0.5570	-0.8059	-0.4117	-0.2103	-0.1074	-0.0549	-0.0280	-0.0143	-0.0073
0.75	2.1048	-0.4797	-0.8338	-0.3800	-0.1732	-0.0790	-0.0360	-0.0164	-0.0075	-0.0034
1	2.0537	-0.4287	-0.8479	-0.3540	-0.1478	-0.0617	-0.0258	-0.0108	-0.0045	-0.0019
2	1.9429	-0.3207	-0.8656	-0.2857	-0.0943	-0.0311	-0.0103	-0.0034	-0.0011	-0.0004
5	1.8256	-0.2118	-0.8637	-0.2004	-0.0465	-0.0108	-0.0025	-0.0006	-0.0001	0
10	1.7585	-0.1524	-0.8529	-0.1478	-0.0256	-0.0044	-0.0008	-0.0001	0	0
100	1.6343	-0.0491	-0.8142	-0.0489	-0.0029	-0.0002	0	0	0	0
∞	1.5708	0	-0.7854	0	0	0	0	0	0	0

TABLE 5

H*	Auxiliary Moment Parameters O_n						
	O_0	O_1	O_2	O_3	O_4	O_5	O_6
0	0.7854	0.7854	-0.3927	0	0	0	0
0.25	0.6864	0.7743	-0.4638	0.0318	0.0123	0.0066	0.0022
0.50	0.7002	0.7675	-0.5163	0.0536	0.0166	0.0053	0.0016
0.75	0.7014	0.7625	-0.5375	0.0698	0.0238	0.0047	0.0010
1	0.7061	0.7586	-0.5531	0.0775	0.0189	0.0040	0.0009
2	0.7351	0.7482	-0.5876	0.1088	0.0173	0.0015	-0.0002
5	0.8253	0.7342	-0.6265	0.1614	0.0093	-0.0024	-0.0011
10	0.9477	0.7231	-0.6485	0.1918	-0.0013	-0.0034	-0.0011
100	0.5074	0.7014	-0.6667	0.2684	-0.0260	-0.0043	-0.0002
∞	0.4909	0.6872	-0.6872	0.2945	-0.0491	0	0

These solutions agree exactly with the accurate modified linearized solutions for an arbitrary form hydrofoil given in the author's previous work [10]. If the correction factor J can be assumed to be unity, these solutions agree with the Tulin-Burkhart solutions [11].

For a special limiting case of $H^* \rightarrow 0$, $\delta \rightarrow 0$,

$$C_L = \frac{\pi}{J} \left(A_0 + \frac{A_1}{2} \right) \quad (29)$$

$$C_D = \frac{\pi}{J} A_0^2 \quad (30)$$

$$C_M = \frac{\pi}{4J^2} \left(A_0 + A_1 - \frac{A_2}{2} \right) \quad (31)$$

If $J = 1$, the solutions agree with those for a planing craft [12]. It may be observed that, in this case, the drag coefficient C_D is connected only with the shape parameter A_0 ; (the drag corresponds to the so-called spray drag [12]).

For a special case of the flat plate hydrofoil,

$$C_L = \frac{\pi}{J} A a_1 A_0 \quad (32)$$

$$C_D = \frac{\pi}{J} A_1 a_1 A_0^2 \quad (33)$$

$$C_M = \frac{\pi a A^2}{J^2} \left\{ \frac{1}{4a} (1 - 4aa_1) + a_1 \ln 4aa_1 + \sum_{\lambda=1}^{\infty} \frac{a_1^{2\lambda+1}}{\lambda(\lambda+1)} \right\} A_0 \quad (34)$$

These seem to agree with Green's exact solutions [1] up to second order terms, when compared on the basis of spray sheet thickness (see the Appendix). If $J = 1$, they agree with the solutions of Auslaender [3] and Hsu [13].

IV. RESTRICTIONS FOR THE FOIL SHAPE PARAMETERS A_n

In this section the restrictions upon the foil shapes or the incidence angles, that is, the parameters A_0 and A_n , are discussed. A physically meaningful solution should satisfy at least the following two conditions.

1. The absolute value of the surface velocity on the pressure side $|q_s|$ not only needs to be less than that of the cavity surface velocity (the assumed magnitude of which is unity) to avoid cavitation on the pressure side, but also needs to be more than zero. As the lift force on a supercavitating foil is induced only by the positive pressure p_s on the pressure side of the foil, it follows from the condition $|q_s| \geq 0$ (that is, $p_s \max \leq \frac{1}{2}\rho q_\infty^2$) that there exists a maximum lift coefficient $C_{L \max}$ for each hydrofoil. In the limiting case of $q_s = 0$, $p_s = \frac{1}{2}\rho q_\infty^2$ over the entire chord, $C_{L \max} = 1$.
2. The distance between the vacuum-side free streamline and the foil surface line, that is, the so-called cavity thickness, should be positive¹ at any point along the chord.

¹For example, the cavity thickness of Tulin's profile ($A_0 = 0$) [11], which partly satisfies condition 1, is largely negative over the chord. Also the actual performance is quite different from that predicted because of an increased incidence angle to insure positive cavity thickness over the chord. Consequently, the predicted performance of Tulin's profile ($A_0 = 0$) seems to be quite meaningless physically.

The author believes that any discussions or any theoretical results ignoring these two important physical conditions for a given arbitrary shape hydrofoil operating at an arbitrary submergence are quite meaningless until these conditions have been checked.

Condition 1 can be checked easily. For the shape parameters A_0 and A_n the surface velocity distribution expressed by Eq. (16") can be obtained by simple harmonic analysis (cosine series). Although condition 1 has been checked by several investigators [5][9][11] in the course of their work, there still remain some interesting problems concerning it. For example, this condition refutes the possibility of Weiker's idea [14] that C_L be finite while $C_D = 0$ for the S-camber hydrofoil ($A_2 \neq 0$, $A_0 = A_3 = A_4 = \dots = 0$ at $H^* = \infty$).

To check condition 2 the suction-side free-streamline shape y_f must be calculated through a rather complicated procedure; consequently most previous studies have either ignored it or performed a very superficial calculation. The following paragraphs describe the calculation of the free-streamline shape y_f .

A. Case of Shallow Submergence

Generally speaking, the shallower the submergence ($H^* < 1$), the more influential the submergence effects are on the foil performance [1][2]. Thus, it is necessary to calculate many points in $H^* < 1$ in order to define the relationship.

The free-streamline shape y_f may be expressed as follows:

$$y_f = \int_0^{x_s} v_f ds = -A \sum_0^{\infty} A_n \int_0^{-\xi_s} \frac{I_n \xi}{a+\xi} d\xi \quad (35)$$

To simplify the relation, for shallower submergence, consider that $H^* < 1$, $a \ll 1$, $|\xi_s| \ll 1$, and let $I_n(\xi_s) \cong \bar{I}_n(-a)$. Therefore, y_f may be expressed approximately by the following straight lines:

$$y_f = \left\{ \sum_0^{\infty} A_n \bar{I}_n (a) \right\} x \quad (35')$$

where

$$\bar{I}_0 = \sqrt{\frac{a+1}{a}} - 1, \quad \bar{I}_1 = \bar{t} - \sqrt{\bar{t}^2 - 1}, \quad \bar{I}_2 = 2\bar{t} \bar{I}_1 - 1;$$

$$\bar{I}_{n+1} = 2\bar{t} \bar{I}_n - \bar{I}_{n-1}, \quad \bar{t} = 2a + 1$$

Practically speaking, the factor $\sum_0^{\infty} A_n \bar{I}_n$ is the vertical velocity component on the spray jet at infinity, or approximately the spray angle¹ τ . That Eq. (35') is sufficiently accurate for the flat plate (where $A_0 \neq 0$, $A_{n \neq 0} = 0$) is demonstrated in Fig. 4 where it may be seen that the smaller H^* is, the better the accuracy is. The accuracy for the parameters A_n ($n \neq 0$) seems to be better, for the shapes of the free streamlines y_f are closer to being straight lines when calculated by Eq. (35) as shown in Fig. 10. The nature of \bar{I}_n in Eq. (35') is shown in Fig. 5 for several typical shape parameters A_n ($\bar{I}_n = \frac{\tan \tau_n}{A_n}$ for each A_n). It is apparent from this figure that there is an exceptionally large spray angle τ_0 for the flat plate ($n = 0$). Also there is a tendency for $\left| \frac{d\tau_n}{dH^*} \right|$ to approach zero rapidly with an increase in the submergence H^* and the subscript n of A_n . Therefore, hydrofoils having higher n -terms of A_n (that is, hydrofoils greatly cambered at the leading and/or the trailing edge) might be expected to have flat C_L vs H^* performance (except for the extreme case of $H^* \approx 0$).

¹The tangential component $1+u_s$ is close to unity.

B. Case of Deeper Submergence

The accuracy of Eq. (35') deteriorates with an increase in the submergence H^* ; consequently Eq. (35') would be of no use for $H^* > 1$. However, for such cases, Eq. (35) is still applicable. After several trial calculations the following fairly accurate representation for y_f was found:

$$y_f \cong -A \int_0^{-x_s} (A_0 I_0 + A_1 I_1 + A_2 I_2) \frac{\xi}{a+\xi} d\xi$$

$$= A_0 y_{fA_0} + A_1 y_{fA_1} + A_2 y_{fA_2} \quad (35'')$$

The values y_{fA_0} , y_{fA_1} , and y_{fA_2} are tabulated in Table 6. Furthermore, the form y_f for $x_s > 0.5$, and y_{fA_n} ($n > 2$) are very close to straight lines parallel to the ones defined by Eq. (35'). Using Eq. (35''), calculations to check condition 2 may be performed very easily.

V. EXISTENCE OF ZERO FORM-DRAG HYDROFOILS

Many investigators have explored the possibility of using a supercavitating hydrofoil in high speed machinery. At present, however, the application to such machinery is extremely limited. The main reason for this is believed to be lower efficiency associated with high drag-lift ratio. Uneconomical performance has been considered inevitable for hydrofoils with rather large trailing cavities and rather large wakes. In this section, however, it is shown that uneconomical performance may be eliminated for hydrofoils operating near a free surface; however, the submergence effects on hydrofoil performances may be extremely large.

The lift and drag coefficients C_L and C_D , at small submergences of $H^* \rightarrow 0$, are shown in Eqs. (29) and (30). In these equations, if $A_0 = 0$ without restriction on the other A_n , quite general hydrofoil shapes may be obtained with the lift coefficient $C_L \cong \frac{\pi}{2} A_1$, and the drag coefficient

TABLE 6

Auxiliary Free Streamline Shape Parameters y_{fA_n}

$H^* = 1.0$				$H^* = 2.0$			
x_s	y_{fA_0}	y_{fA_1}	y_{fA_2}	x_s	y_{fA_0}	y_{fA_1}	y_{fA_2}
0	0	0	0	0	0	0	0
0.01	0.0515	0.0071	0.0050	0.01	0.0463	0.0068	0.0046
0.02	0.0851	0.0133	0.0089	0.02	0.0760	0.0128	0.0083
0.03	0.1141	0.0193	0.0124	0.03	0.1015	0.0185	0.0115
0.05	0.1655	0.0306	0.0189	0.05	0.1461	0.0289	0.0169
0.07	0.2118	0.0412	0.0245	0.07	0.1857	0.0389	0.0220
0.10	0.2754	0.0567	0.0325	0.10	0.2397	0.0531	0.0287
0.20	0.4625	0.1050	0.0558	0.20	0.3949	0.0968	0.0478
0.30	0.6311	0.1539	0.0831	0.30	0.5309	0.1373	0.0642
0.40	0.7906	0.1951	0.0965	0.40	0.6567	0.1758	0.0790
0.50	0.9448	0.2387	0.1155	0.50	0.7761	0.2133	0.0931
0.60	1.0957	0.2816	0.1339	0.60	0.8911	0.2498	0.1064
0.70	1.2443	0.3243	0.1521	0.70	1.0028	0.2831	0.1142
0.80	1.3914	0.3667	0.1701	0.80	1.1121	0.3145	0.1189
0.90	1.5374	0.4089	0.1879	0.90	1.2194	0.3559	0.1440
0.95	1.6101	0.4299	0.1968	0.95	1.2725	0.3733	0.1500
1.00	1.6827	0.4510	0.2057	1.00	1.3252	0.3904	0.1557

$H^* = 5.0$				$H^* = \infty$			
x_s	y_{fA_0}	y_{fA_1}	y_{fA_2}	x_s	y_{fA_0}	y_{fA_1}	y_{fA_2}
0	0	0	0	0	0	0	0
0.01	0.0416	0.0067	0.0046	0.0045	0.0191	0.0030	0.0020
0.02	0.0678	0.0123	0.0077	0.0137	0.0415	0.0080	0.0047
0.03	0.0902	0.0176	0.0105	0.0319	0.0740	0.0166	0.0088
0.05	0.1289	0.0273	0.0151	0.0625	0.1162	0.0291	0.0139
0.07	0.1630	0.0365	0.0193	0.1082	0.1669	0.0454	0.0197
0.10	0.2089	0.0496	0.0251	0.1707	0.2245	0.0651	0.0259
0.20	0.3382	0.0887	0.0402	0.2500	0.2868	0.0874	0.0322
0.30	0.4485	0.1242	0.0528	0.3444	0.3514	0.1115	0.0384
0.40	0.5486	0.1577	0.0643	0.4503	0.4160	0.1362	0.0443
0.50	0.6418	0.1895	0.0745	0.5625	0.4779	0.1605	0.0494
0.60	0.7300	0.2200	0.0834	0.6747	0.5348	0.1832	0.0540
0.70	0.8146	0.2497	0.0923	0.7797	0.5846	0.2033	0.0578
0.80	0.8961	0.2787	0.1007	0.8705	0.6254	9.2200	0.0609
0.90	0.9753	0.3070	0.1087	0.9406	0.6557	0.2324	0.0632
0.95	1.0141	0.3209	0.1125	0.9849	0.6744	0.2402	0.0645
1.00	1.0524	0.3347	0.1162	1.0000	0.6807	0.2427	0.0649

$C_D \approx 0$, if the surface pressure on the pressure side and the cavity thickness¹ may be made positive over the chord. Also, there is a maximum value of C_L determined by condition 1 on page 14 (see Ref. [9]) which cannot be exceeded; this will be called $C_{L \max}$.

Figure 6 shows the profile y_s , the free streamline y_f , and the surface velocity distribution u_s/A_1 of the so-called \bar{A}_1 -hydrofoil ($A_1 \neq 0$, $A_0 = A_2 = A_3 = \dots = 0$) operating in the neighborhood of $H^* = 0$. As seen in Fig. 6, the cavity thickness and the surface pressure are positive over the chord. If C_L is restricted to $C_L < C_{L \max}$ (or $A_1 < A_{1 \max}$), the necessary and sufficient conditions 1 and 2 for supercavitating flow are satisfied completely. Here, theoretically, one could find a zero form-drag hydrofoil of $C_L = \frac{\pi}{2} A_1$ (finite) and $C_D \approx 0$. For the hydrofoil defined by $A_2/A_1 = 0.5$, $A_1 \neq 0$, $A_2 \neq 0$, $A_0 = A_3 = A_4 = \dots = 0$ at $H^* = 0$, the cavity thickness and the surface pressure are also positive over the chord, $C_L = \frac{\pi}{2} A_1$ (finite), and $C_D \approx 0$ (see Fig. 7). Thus this hydrofoil is also theoretically a zero form-drag hydrofoil and has a larger included angle at the leading edge than the one for the \bar{A}_1 -hydrofoil. In the same way, an infinite number of zero form-drag hydrofoils might be found. Auslaender [3] also shows the theoretical possibility of the existence of hydrofoils such as $C_D \approx 0$ and $C_L > 0$ (finite) at $H^* = 0$. However, he did not fully consider the necessary and sufficient condition 2 for the supercavitating flow.

Now, the discussion will be extended to the case of arbitrary submergence. To arrive at the approximate tendency in the C_L vs H^* performance or the C_D vs H^* performance, the discussion will first be limited to a special case of $A_1 \neq 0$, $A_0 = A_2 = A_3 = \dots = 0$. For this case,

$$\frac{C_D}{\frac{\pi}{2} A_1^2} = 2Aaa_1^2 \quad (36)$$

$$\frac{C_L}{\frac{\pi}{2} A_1} = A(1 - 4aa_1) \quad (37)$$

As seen in Fig. 8 for this A_1 -hydrofoil family, the lift scarcely changes with depth staying within 3.5 per cent for the whole range of H^* , but the drag

¹Cavity thickness is defined as the difference between the foil surface on the pressure side and the vacuum-side free streamline.

changes greatly. For given lift coefficient, the drag coefficient at $H^* = \infty$ reduces to about 1/2, 1/5, and 0 for $H^* = 1, 0.25,$ and 0 respectively as may be seen in Fig. 8. For the A_1 -hydrofoil, the cavity thickness and the surface pressure are positive over the chord, unless H^* is too large; (if $H^* = \infty$, the cavity thickness becomes slightly negative near the leading edge, as shown in Ref. [9]). Thus the necessary and sufficient conditions 1 and 2 for the supercavitating flow seem to be satisfied unless A_1 is too large. Figure 8 indicates that:

1. The submergence effects on the performance of hydrofoils operating near a free surface are extremely large and cannot be neglected. C_L and C_D at $H^* = 1 \sim 10$ of the practical usable range differ only moderately from C_L and C_D at $H^* = \infty$.
2. The drag coefficient C_D for the A_1 -hydrofoil family rapidly decreases as the submergence $H^* \rightarrow 0$. This peculiar tendency is completely opposite the tendency of the flat plate. C_L scarcely changes in this range also.

The A_1 -hydrofoil is a special shape and the above discussion is not necessarily relevant to a general discussion of submergence effects on hydrofoil performance. To increase the generality, define two typical cambered hydrofoils, for example, the SH1 and the SH2 hydrofoils¹, made up of circular arc shapes ($A_1 \neq 0, A_0 = A_2 = A_3 = \dots = 0$ at $H^* = 0$), S-shapes ($A_2 \neq 0, A_0 = A_1 = A_3 = A_4 = \dots = 0$ at $H^* = 0$), and flat inclined shapes ($A_0 \neq 0, A_1 = A_2 = \dots = 0$) for the purpose of satisfying the necessary and sufficient condition 2 for the supercavitating flow. The ratio A_2/A_1 for SH1 or SH2 is taken as -1/2 or 1/2 respectively, while $A_0 = 0$. Performance is shown in Fig. 9. The hydrofoil shapes y_s and the suction-side free streamline shapes y_f are shown in Fig. 10, while the surface velocity distributions u_s are shown in Fig. 11. These figures indicate that:

1. The C_L vs H^* , the C_D vs H^* , and the C_D/C_L performances vary to a considerable degree with the hydrofoil shape.
2. Three quite different types of behavior are present in the C_D vs H^* performance: one in which

¹The performance of the SH2 hydrofoil was also discussed in the previous section (see Fig. 7).

- C_D decreases with an increase in H^* , as in the flat plate; the second in which C_D is quite level over H^* except in the neighborhood of $H^* = 0$, as in the SH1 hydrofoil; and the third in which C_D increases with H^* , as in the SH2 Hydrofoil.
3. The change in C_L due to change in submergence is attributable principally to the change in the surface pressure on the forepart of the foil, $x_s < 0.5$ (see Fig. 11).
 4. The C_L vs H^* performance of the SH1 hydrofoil is especially interesting since C_L is approximately constant for $H^* > 2$.
 5. The results for C_D vs H^* and C_D/C_L obtained for the A_1 -hydrofoil family are apparently verified for these somewhat more complicated shapes.

For both SH1 and SH2 hydrofoils the necessary and sufficient conditions 1 and 2 for supercavitating flow are completely satisfied except for the extreme submergence range of $H^* > 5$ (for SH1) and $H^* \approx \infty$ (for SH2) respectively, if $C_L < C_{L \max}$.

Johnson [5] discusses in his approximate theory the camber effects upon the C_L vs H^* performance. However, he did not fully consider the physically necessary and sufficient conditions for supercavitating flow. Generally speaking, every supercavitating hydrofoil has its original minimum incidence angle [9], α_{\min} (and $A_{o \min}$), to satisfy condition 2. As seen in Fig. 9, the submergence effects for the lift coefficient on a flat plate are quite large. Therefore, it is apparent that Johnson's results should be modified to include the effect of submergence on C_{LA_o} and to satisfy condition 2.

VI. THE EXISTENCE OF HYDRODYNAMICALLY STABLE HYDROFOILS OPERATING NEAR A FREE SURFACE

Most of the known two-dimensional supercavitating hydrofoils (for example, the flat plates, the SH1 hydrofoil, the SH2 hydrofoil, the circular arc hydrofoil, the Tulin hydrofoils, and the flapped hydrofoil) are hydrodynamically unstable when operated under a free surface, especially at shallow submergence where low form drag is to be expected; that is, the lift decreases

as the submergence becomes greater. Consequently, a supercavitating hydrofoil boat may be unstable in rolling, pitching, and heaving motions.

Of course, several practical methods to provide stability in such hydrofoil boats have been proposed, as for example dihedral foils or control devices. However, no research seeking an inherently hydrodynamically stable hydrofoil form has been reported. In this section, therefore, as the first step in such direction, the theoretical possibility of the existence of such stable two-dimensional supercavitating hydrofoil forms is discussed.

The following discussion is limited to the shallower H^* range in which C_L changes considerably, as shown, for example, in Fig. 9a. First, considering a hydrofoil of approximate circular arc camber ($A_1 \neq 0$, $A_0 = 0.1 A_1$, $A_2 = A_3 = \dots = 0$ at $H^* = 0$) called \bar{A}_1 , the C_L vs H^* performance was calculated and is shown in Fig. 12. This figure also shows the hydrofoil shape y_s , the suction-side free streamline shape y_f , and the surface velocity distribution u_s . The restriction $A_0 = 0.1 A_1$ resulted from the necessary and sufficient condition 2 for the supercavitating flow. As can be seen in Fig. 12, if the restriction $C_L < C_{L \max}$ is used, the \bar{A}_1 -hydrofoil completely satisfies the necessary and sufficient conditions 1 and 2, in the working range of $H^* < 1$.

In Fig. 12, the C_L vs H^* performance, although it still has unstable characteristics, is much better than the performance of the flat plate. The improvement in the C_L vs H^* performances probably correspond to the large difference in the surface velocity distributions which may be seen by comparing Fig. 12b with Fig. 13 for the flat plate. Since the change in C_L due to H^* principally corresponds to the change in the surface velocity in the fore part of the foil, as shown in Figs. 12b and 13, it is quite natural that the change in C_L is exceptionally large for the flat plate in which velocity distribution is one-sided toward the front, and fairly small for the \bar{A}_1 -hydrofoil (in which velocity distribution is approximately level). Furthermore, the large difference in the C_L vs H^* performances may correspond to the large differences in the spray angle τ shown in Fig. 5; (the change in C_L corresponds to the change in momentum difference between the upstream infinity and downstream infinity, that is, to the product $H^* \times \tau$).

Returning to the C_L vs H^* performance of the \bar{A}_1 -hydrofoil, if the narrower working range of $H^* < 0.25$ is selected, the most severe restriction

on the cavity thickness (condition 2) may be greatly reduced, and consequently the C_L vs H^* performance may be improved as shown in Fig. 12c. At the limiting condition $H^* \rightarrow 0$, the C_L vs H^* curve tends to a maximum value of C_L . Hence, this \bar{A}_1 -hydrofoil does not have a stable characteristic, even in the limiting case.

The performance calculated for an \bar{A}_2 -hydrofoil of a typical S-camber ($A_2 < 0$, $A_0 = A_1 = A_3 = \dots = 0$ at $H^* = 0$) is shown in Fig. 14. With a locally negative cavity thickness and negative static pressure as shown in Fig. 14, the \bar{A}_2 -hydrofoil itself is physically meaningless, although it possesses a stable lift characteristic. However, a physically meaningful hydrofoil can be obtained by combining the \bar{A}_2 -hydrofoil with a known hydrofoil.

In an attempt to combine the \bar{A}_2 -hydrofoil and \bar{A}_1 -hydrofoil, $\left. \frac{A_1}{A_2} \right|_{H^*=0} = 1$ is assumed for the camber to simplify the problem. In the combined hydrofoil shown in Figs. 12 and 14 the necessary and sufficient conditions 1 and 2 for supercavitating flow are completely satisfied in the working range of $0 < H^* < H_0^*$, where $H_0^* < 0.25$. It should be remembered that the C_L vs H^* performance of the \bar{A}_1 -hydrofoil tends to a critical line of $C_L = \text{const.}$ in a limiting case of $H^* \rightarrow 0$, and also that the \bar{A}_2 -hydrofoil has a stable performance. Hence, a theoretical possibility of existence of hydrodynamically stable C_L vs H^* performance is found in the combined hydrofoil.

The above discussion covers only two elementary hydrofoils, \bar{A}_1 and \bar{A}_2 , and only one combination ratio, 1:1. By using more elementary hydrofoils, \bar{A}_3 , \bar{A}_4 , . . . , and more combination ratios, an infinite number of hydrodynamically stable hydrofoils can be obtained by the method discussed above.¹ Furthermore, as indicated in Fig. 5 (which shows the change in the spray angle τ due to changes in H^*), the larger the suffix number n of A_n , the steeper the slope $\frac{\partial \tau_n}{\partial H^*}$ at $H^* = 0$. Therefore, a larger n can be expected to improve the C_L vs H^* performance in the elementary hydrofoils \bar{A}_3 , \bar{A}_4 ,

¹Even if the cavity thickness locally becomes negative, the thickness can be increased with very small effect on the C_L vs H^* performance by means of slightly increasing A_0 , under an assumption of very small submergence H (see Fig. 15).

VII. CONCLUSIONS

The results obtained in this paper may be summarized as follows:

1. An accurate method of estimating the performance of two-dimensional supercavitating hydrofoils of quite arbitrary form operating at quite arbitrary submergence (direct method) through improvement of Johnson's approximate method [5] was proposed. This analysis was based on the following two physically necessary and sufficient conditions for insuring supercavitating flow around the foils:
 - (i) The absolute value of the surface velocity on the pressure side not only needs to be less than that of the cavity surface velocity to avoid occurrence of cavitation on this side, but also needs to be more than zero.
 - (ii) The distance between the vacuum-side free streamline and the pressure-side foil surface line, that is, the so-called cavity thickness, should be positive at any point along the chord.

The analysis proposed above may also be applied to obtain hydrofoil shapes for given surface velocity distributions (inverse method) without any modification.
2. The existence of hydrodynamically stable hydrofoils in which the lift coefficient increases as the submergence becomes greater, in the shallower submergence range, was found theoretically possible.
3. An infinite number of zero form-drag supercavitating hydrofoils of finite lift coefficient C_L ($C_L < C_{L \max} < 1$, where $C_{L \max}$ has a specific value for each hydrofoil) should exist.
4. The relation between lift coefficient and submergence varies considerably among hydrofoil shapes. For example, in the flat plate hydrofoil, C_L at $H^* = 0$ is double its value at $H^* = \infty$, while, in the A_1 -hydrofoil of an approximate circular arc camber, C_L changes very little in the same working range of $0 < H^* < \infty$ (see Figs. 8, 12, and 14).
5. The change in C_L due to change in submergence corresponds to the change in the surface velocity on the front half of the foil. Therefore, it is quite natural that the change in C_L is exceptionally large for the flat plate, in which the

surface velocity distribution is one-sided toward the front half of the foil, and fairly small for the A_1 -hydrofoil, in which the surface velocity distribution is almost flat (see Fig. 12). Therefore, it may be expected that the more distorted the hydrofoil camber is toward the rear half of the foil, the less C_L will change.

6. Depending on shape of hydrofoil, any one of three different relationships may exist between drag coefficient and submergence: one in which C_D decreases with an increase in H^* as in the flat plate, the second in which C_D is constant except in the immediate neighborhood of $H^* = 0$ as in the SH1 hydrofoil, and the third in which C_D increases with H^* as in the SH2 hydrofoil (see Figs. 8 and 9).
7. The drag-lift ratio, or rather the relationship between the losses and the effective forces of a hydrofoil, changes considerably with submergence and also with shape as shown in Figs. 8 and 9. For example, in the A_1 -hydrofoil for fixed lift coefficient, the drag coefficient at $H^* = \infty$ reduces to about $1/2$, $1/5$, and $1/\infty$ for $H^* = 1$, 0.25 , and 0 respectively.
8. Changes due to submergence are especially important at the shallower submergences of $H^* < 1$ and are not very important in the practical usable range of $H^* = 1$ to 10 . However, the difference between the forces in the range of $H^* = 1$ to 10 and the ones at $H^* = \infty$, is not necessarily negligibly small as shown in Figs. 8 and 9.
9. To check the accuracy of the present solution, a comparison was made with Green's exact solution [1] for the flat plate operating at an arbitrary submergence as well as the author's second order solution [10] for arbitrary form hydrofoils in infinite fluid. The solution was found sufficiently accurate. It was also found that the present solution includes as special limiting cases Tulin-Burkhart's solution in infinite fluid, Wagner's solution [12] for planing ($H^* = 0$), and Auslaender's [3] and Hsu's [13] solutions for flat plate hydrofoils operating at arbitrary submergences.

ACKNOWLEDGMENTS

This research has been supported by the Office of Naval Research of the United States Department of the Navy under Contract Nonr 710(24), Task NR 062-052.

The author would like to express his cordial appreciation to Professors E. Silberman and C. S. Song, St. Anthony Falls Hydraulic Laboratory, University of Minnesota, for useful discussions and encouragement, and also to Mrs. Mary Marsh and Mr. Alwin C. H. Young for their help. The manuscript was prepared for printing by Marjorie Olson.

LIST OF REFERENCES

- [1] Green, A. E., "Note on the Gliding of a Plate on the Surface of a Stream," Proceedings Cambridge Phil. Society, Vol. 32, Part 2, 1936, p. 248.
- [2] Auslaender, J., "Supercavitating Foils with Flaps Beneath a Free Surface," Journal of Basic Engineering, Transactions ASME, Series D, Vol. 86, 1964, p. 197.
- [3] Auslaender, J., "The Linearized Theory for Supercavitating Hydrofoils Operating at High Speeds Near a Free Surface," Journal of Ship Research, Vol. 6, No. 2, 1962, p. 8.
- [4] Luu, T. S. and Fruman, D., "Hydrodynamics, Method for the Design of Supercavitating Hydrofoil Sections in the Presence of Free Surface," Bureau of Ships (Washington, D. C.) Translation No. 885, November 1964.
- [5] Johnson, V. E. Jr., Theoretical and Experimental Investigation of Supercavitating Hydrofoils Operating Near the Free Water Surface, NASA TR R-93, 1961.
- [6] Riegels, F., "Das Umströmungsproblem bei inkompressiblen Potentialströmungen," Ing. Arch., Bd. 16, 1948, S. 373; Bd. 17, 1949, S. 94.
- [7] Auslaender, J., Low Drag Supercavitating Hydrofoil Sections, Hydronautics Inc., TR 001-7, 1962.
- [8] Ōba, R., "Theory on Supercavitating Hydrofoils at Arbitrary Cavitation Coefficient," Reports Institute of High Speed Mechanics, Japan, Vol. 15, 1963/1964, p. 1.
- [9] Ōba, R., "Linearized Theory of Supercavitating Flow Through an Arbitrary Form Hydrofoil," Zeitschrift für Angewandte Mathematik und Mechanik, Bd. 41, 1961, S. 354.
- [10] Ōba, R., "Theory for Supercavitating Flow Through an Arbitrary Form Hydrofoil," Journal of Basic Engineering, Transactions ASME, Series D, Vol. 86, 1964, p. 285.
- [11] Tulin, M. P. and Burkhart, M. P., Linearized Theory for Flows about Lifting Foils at Zero Cavitation Number, David Taylor Model Basin Report C-638, 1955.
- [12] Wagner, H., Planing of Watercraft, NACA TM No. 1139, 1948 (Translation "Jahrbuch der Schiffbautechnik," Bd. 34, 1933).
- [13] Hsu, C. C., Non-steady Hydrodynamic Characteristics of a Supercavitating Hydrofoil under a Free Surface, Hydronautics Inc. TR 463-2, 1964.
- [14] Weicker, D., "Über Schraubenpropeller für sehr schnelle Schiffe," Schiff und Hafen, Bd. 7, 1959, S. 599.

F I G U R E S
(1 through 16)

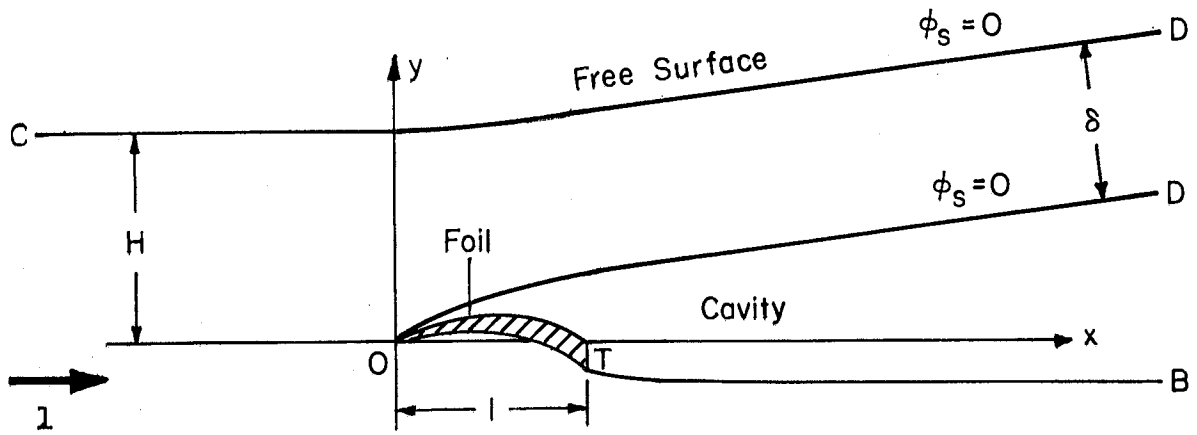


Fig. 1 - Physical Plane, $z = x + iy$

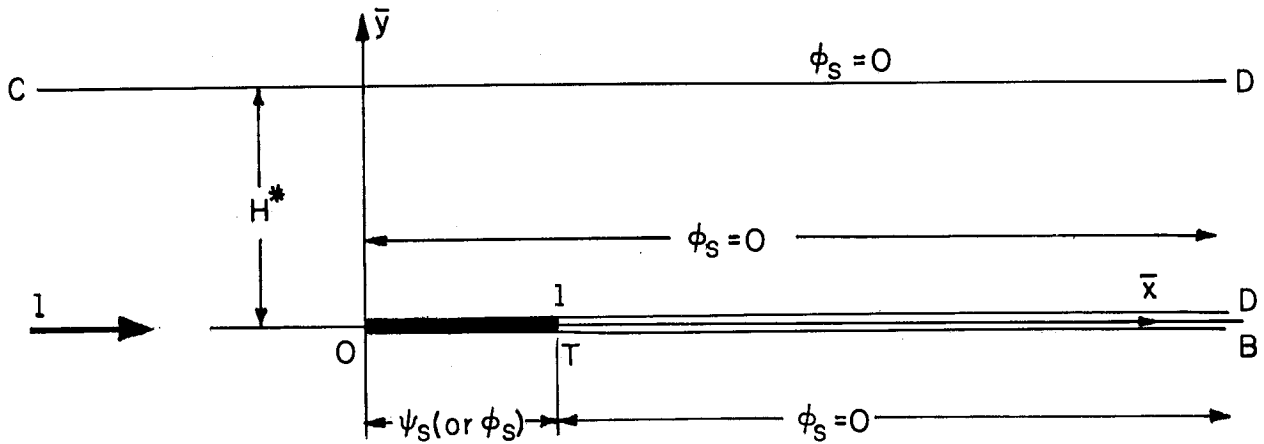


Fig. 2 - Mapping Plane by Riegels' Transformation, $\bar{z} = \bar{x} + i\bar{y}$

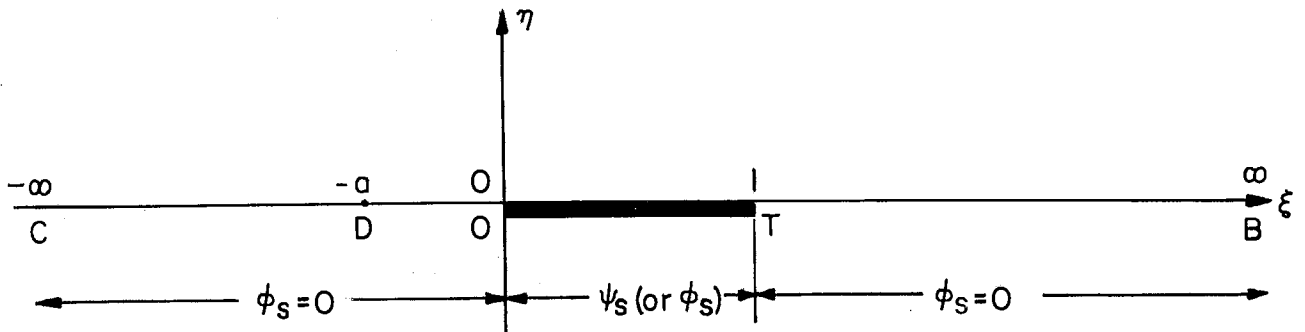


Fig. 3 - Mapping Plane (Lower Half Plane), $\zeta = \xi + i\eta$

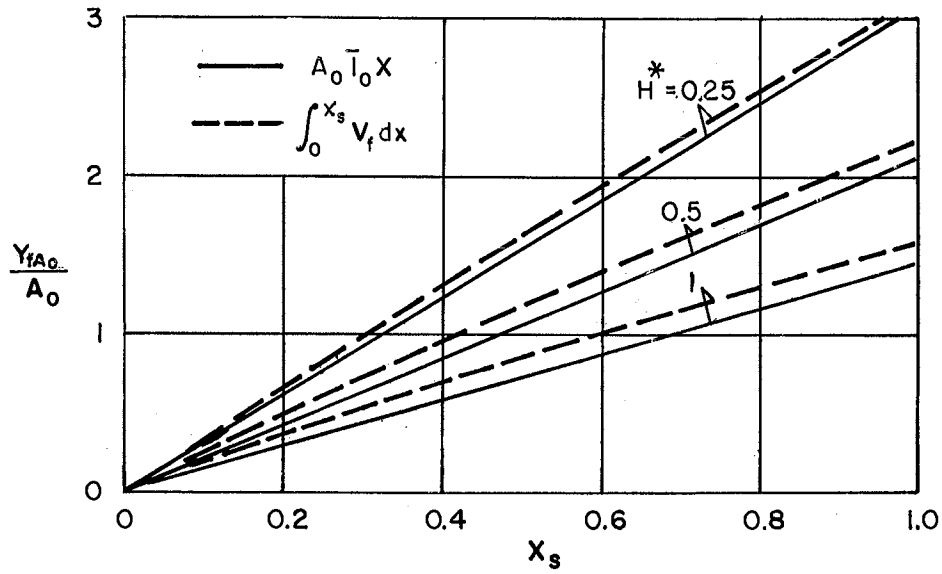


Fig. 4 - Accuracy of Simple Approximation for y_f for Flat Plate;
 $A_0 \neq 0, A_1 = A_2 = \dots = 0$

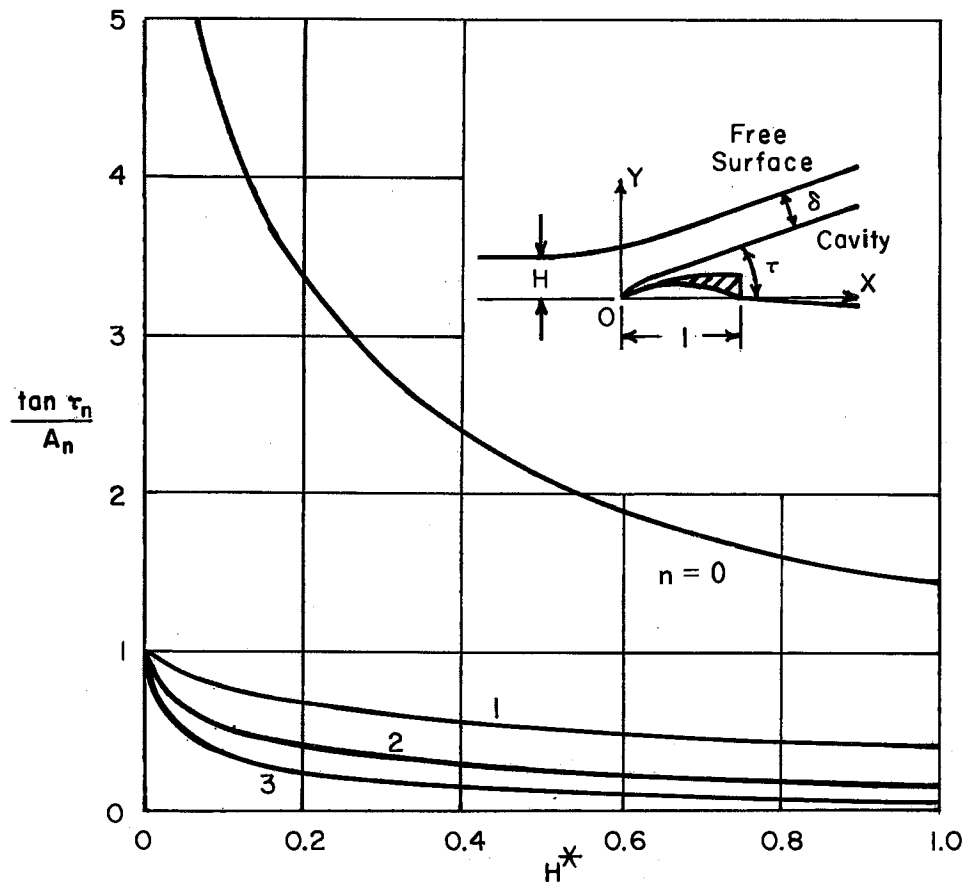


Fig. 5 - Change in Spray Angle τ_n due to Submergence H^* for
 Various Shape Parameters A_n

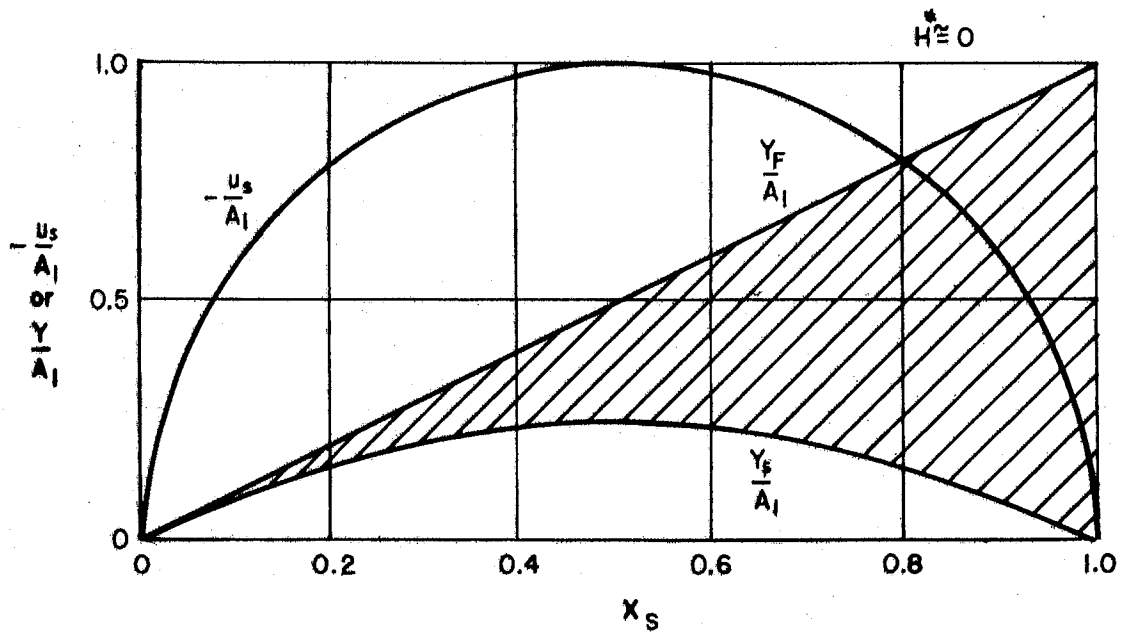


Fig. 6 - Zero Form-Drag Supercavitating Hydrofoil No. 1 at $H^* \approx 0$;
 $C_L \approx \frac{\pi}{2} A_1$, $C_D \approx 0$, ($A_1 \neq 0$, $A_{n \neq 1} = 0$)

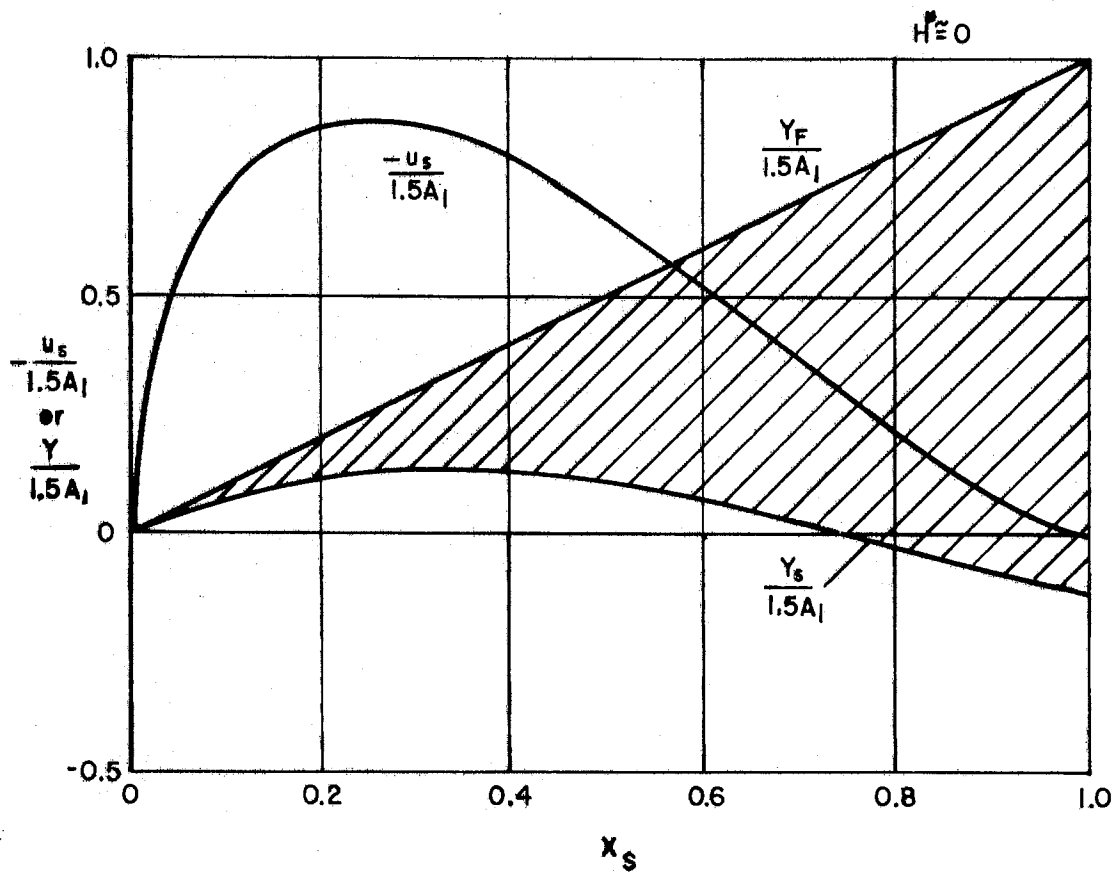


Fig. 7 - Zero Form-Drag Supercavitating Hydrofoil No. 2 at $H^* \approx 0$;
 $C_L \approx \frac{\pi}{2} A_1$, $C_D \approx 0$, ($A_1 \neq 0$, $A_2 \neq 0$, $A_{n \neq 1,2} = 0$)

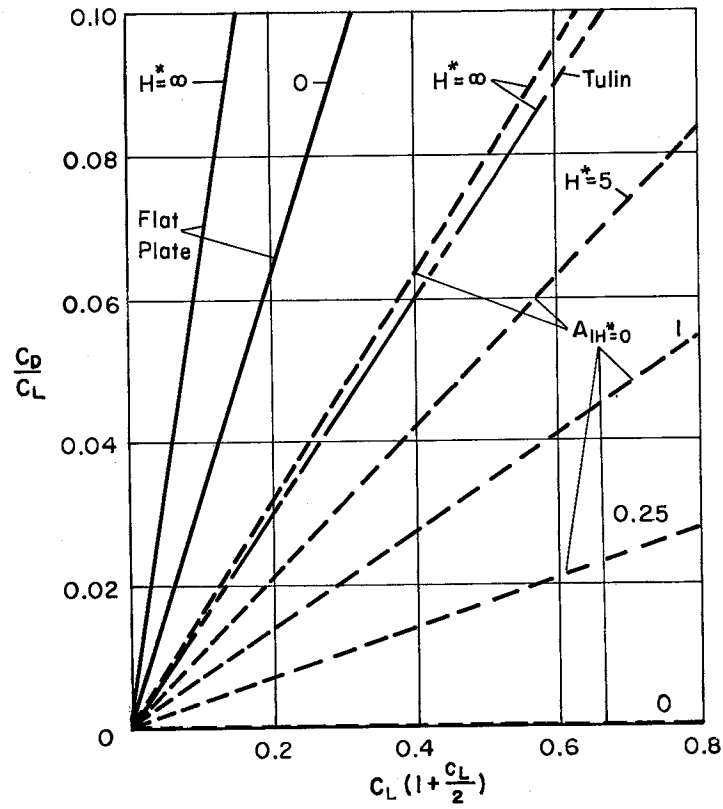
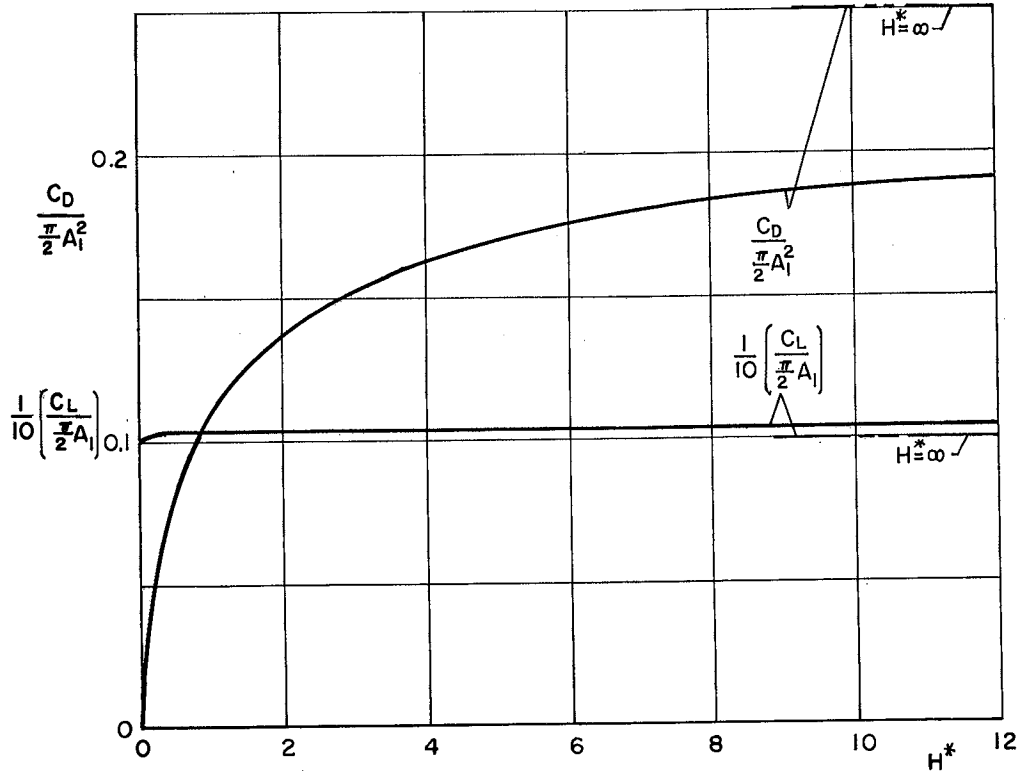


Fig. 8 - Performance of A_1 -Hydrofoil at Deeper Submergence

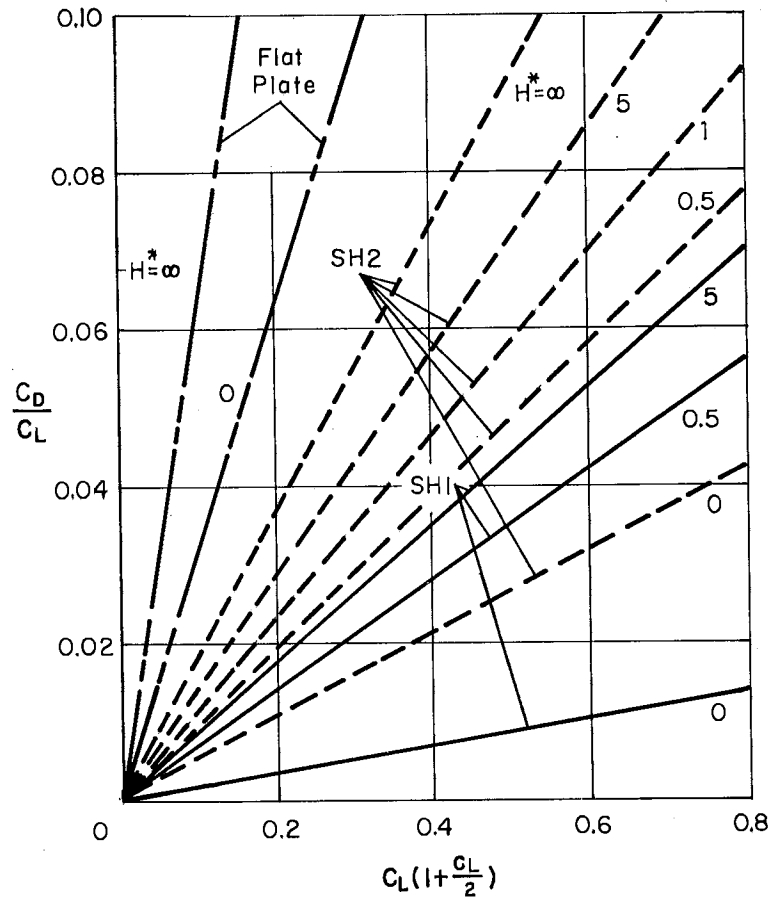
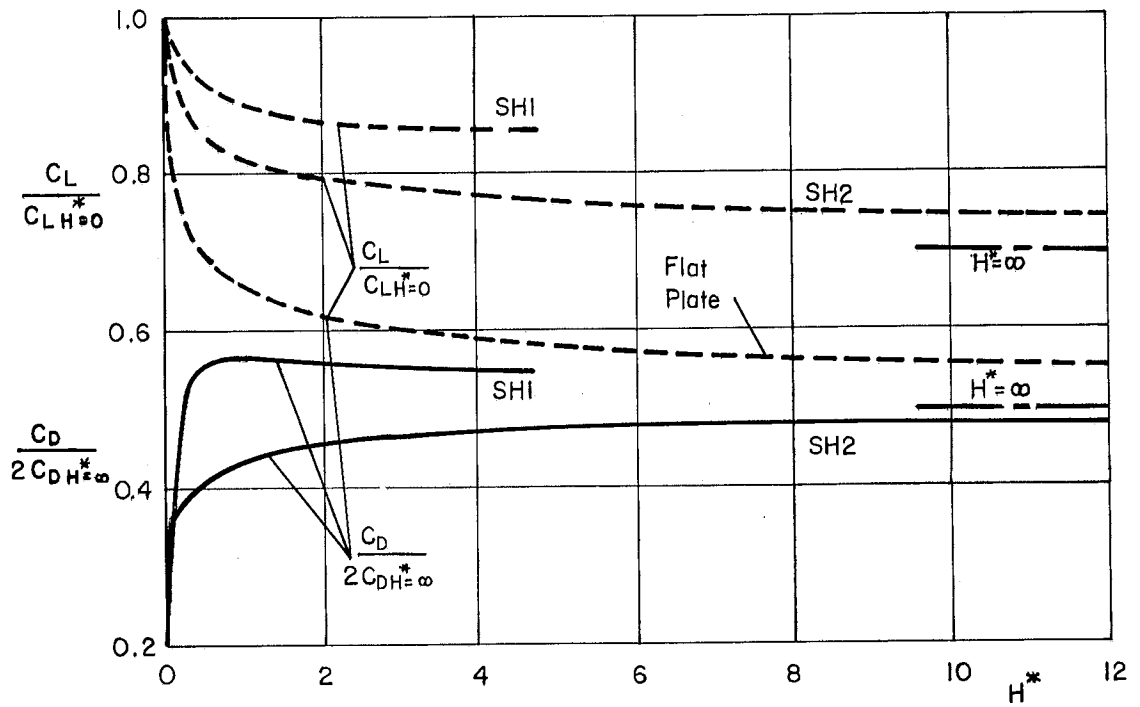


Fig. 9 - Performance of SH1 and SH2 Hydrofoils as a Function of Submergence H^*

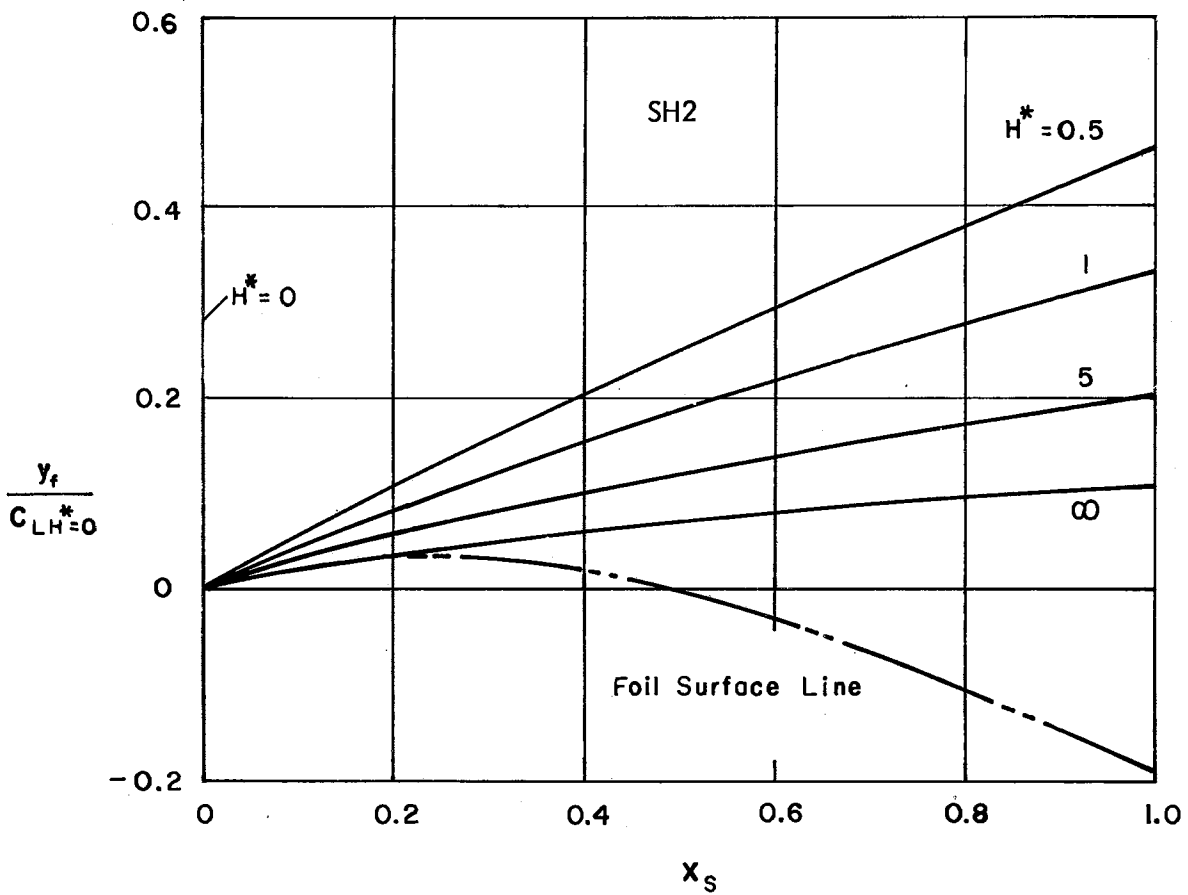
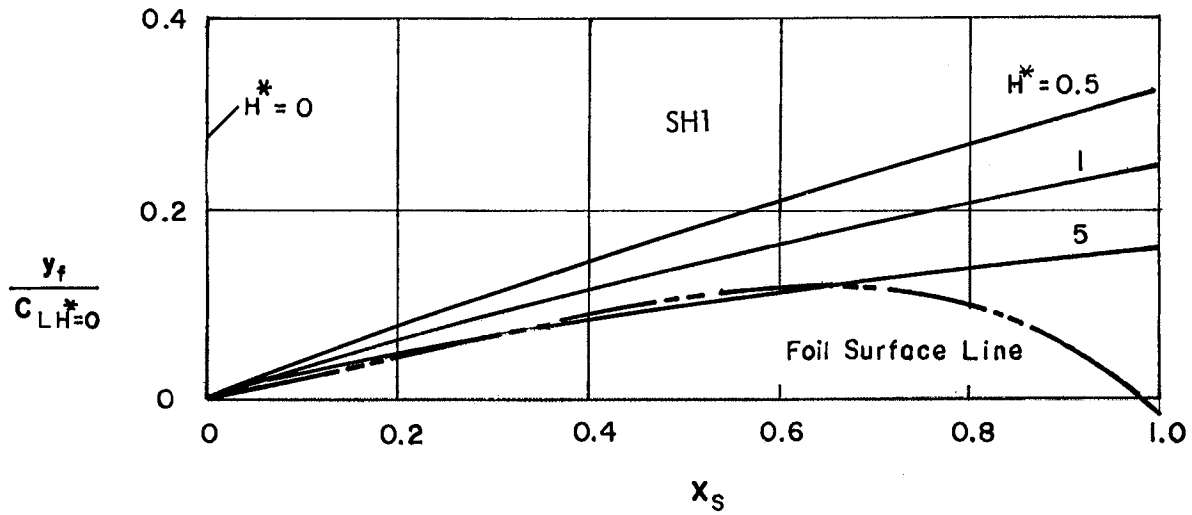


Fig. 10 - Hydrofoil Shapes and Suction-Side Free Streamline Shapes y_f for Various Submergences H^* of SH1 and SH2 Hydrofoils

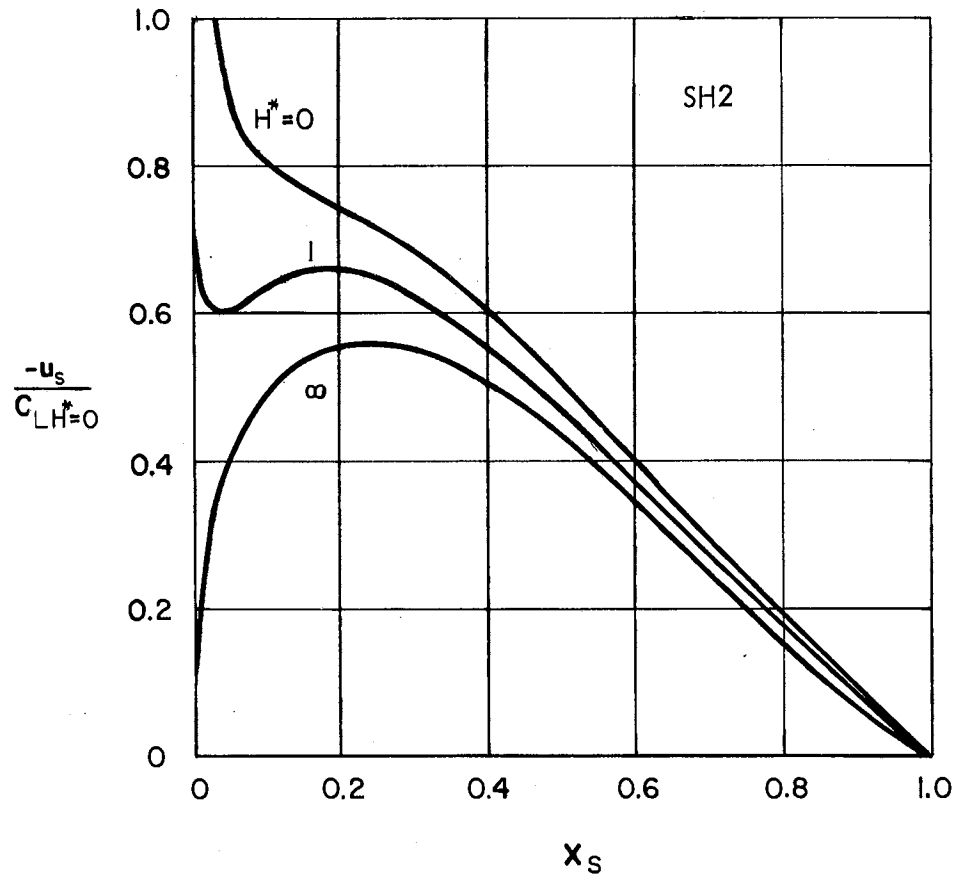
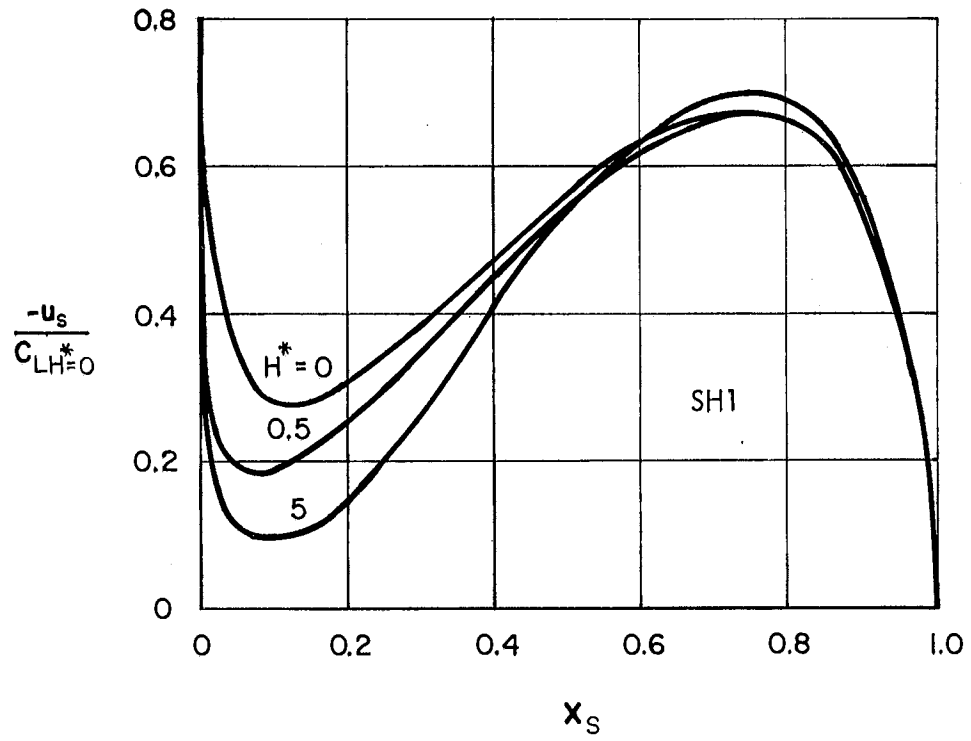


Fig. 11 - Surface Velocity Distribution u_s for Various Submergences H^* of SH1 and SH2 Hydrofoils

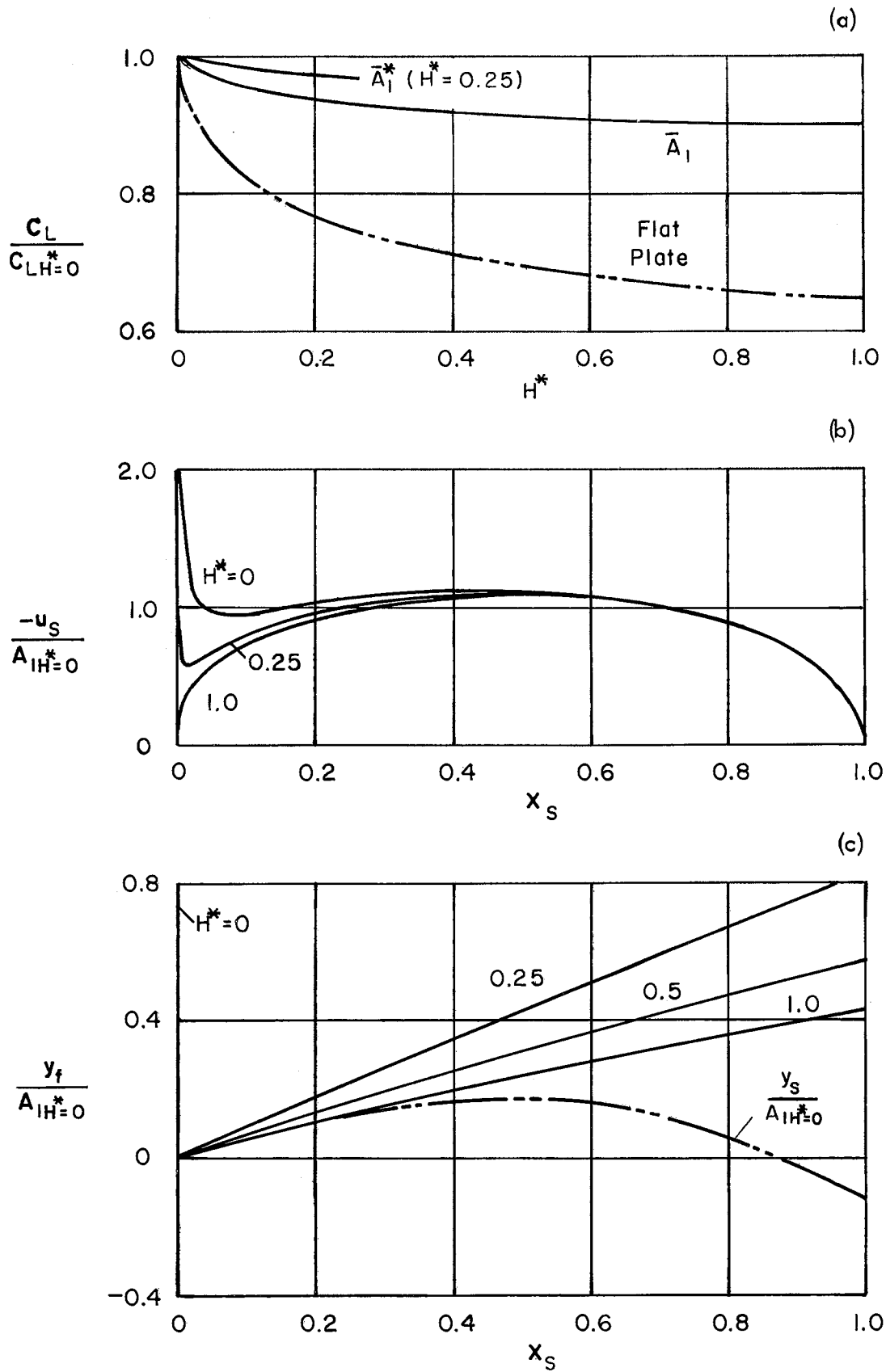


Fig. 12 - Performance of the \bar{A}_1 Approximate Circular Arc Hydrofoil

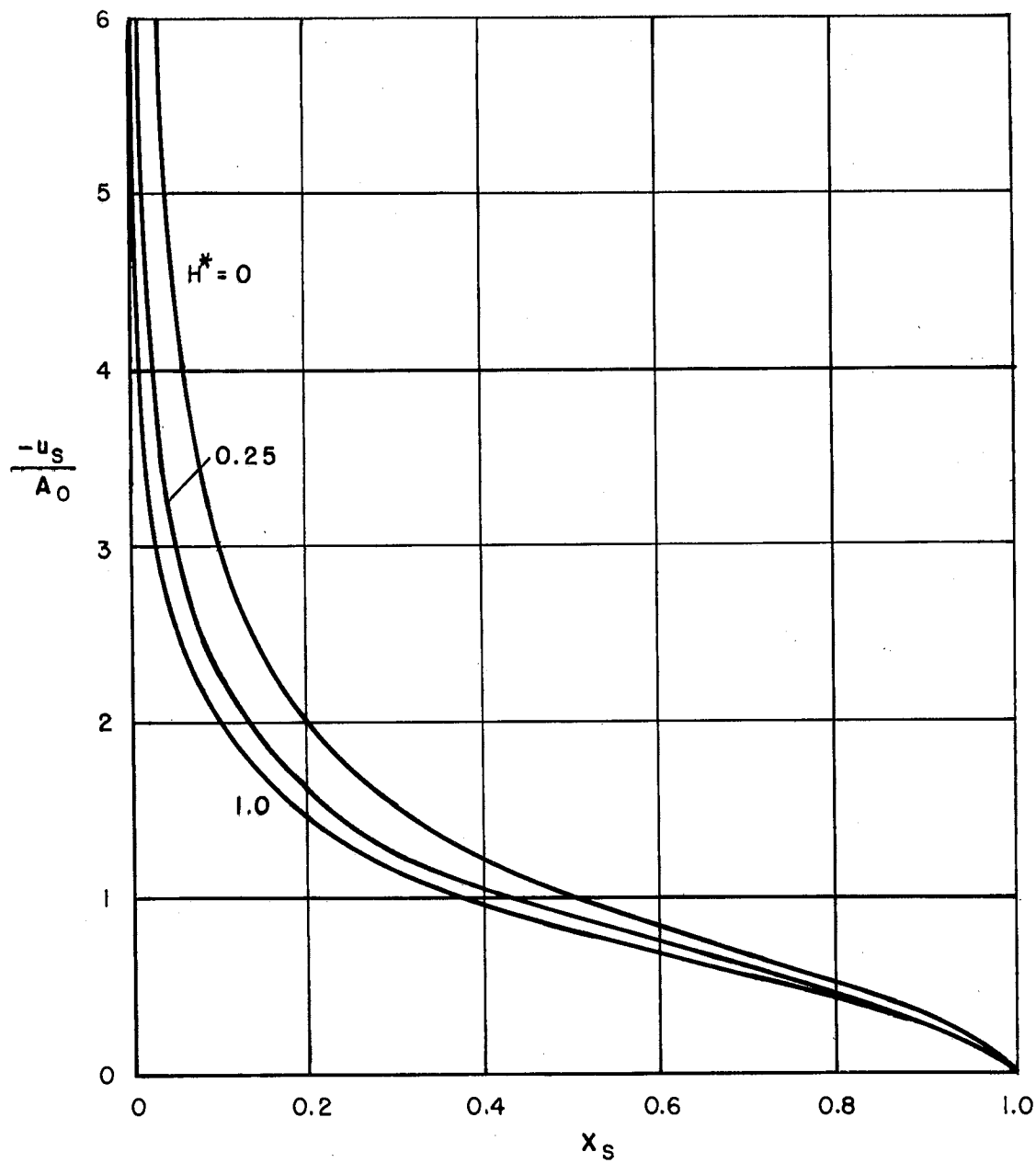


Fig. 13 - Surface Velocity Distribution u_s of the Flat Plate Hydrofoil

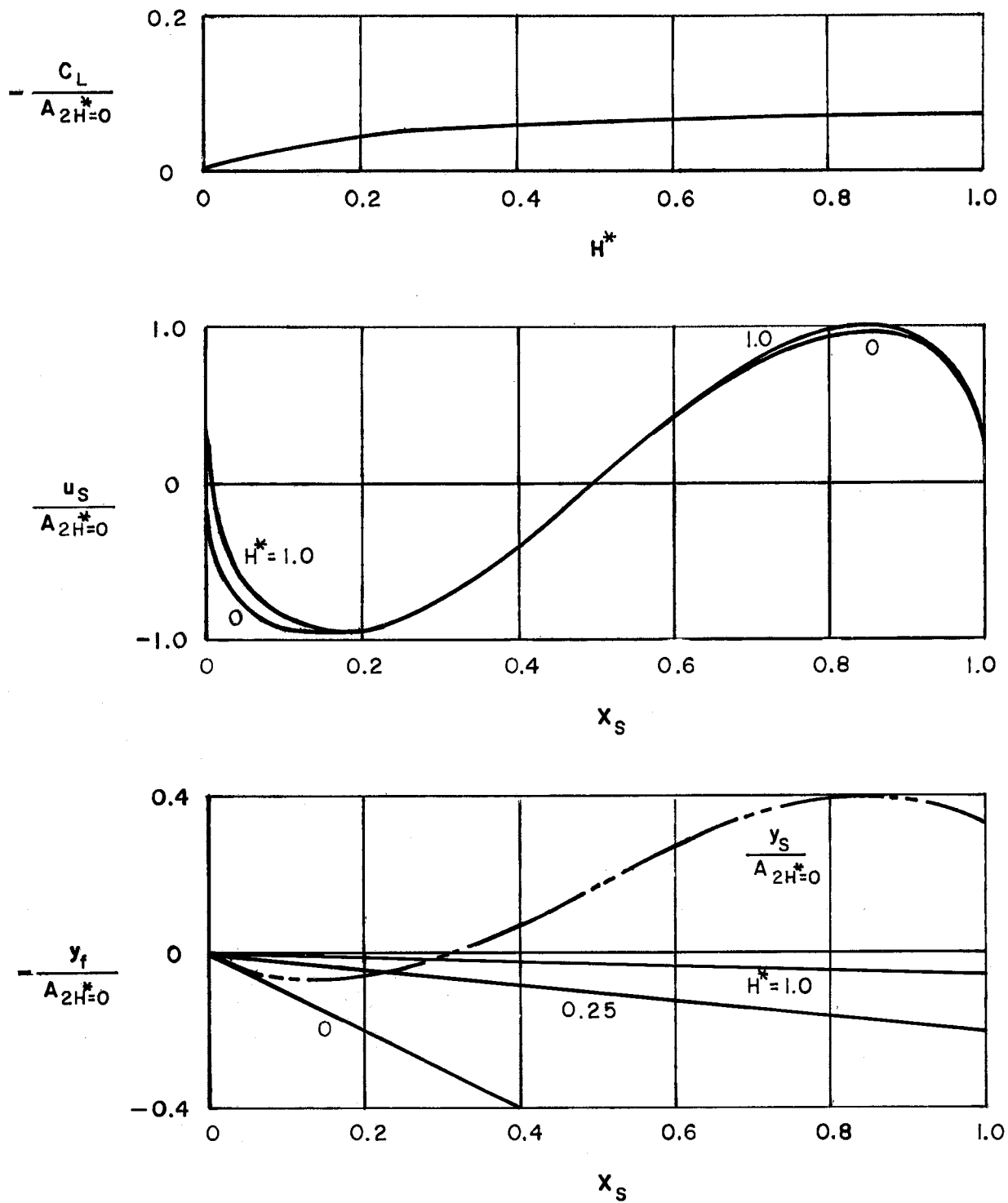


Fig. 14 - Performances of the \bar{A}_2 , S-Cambered Hydrofoil

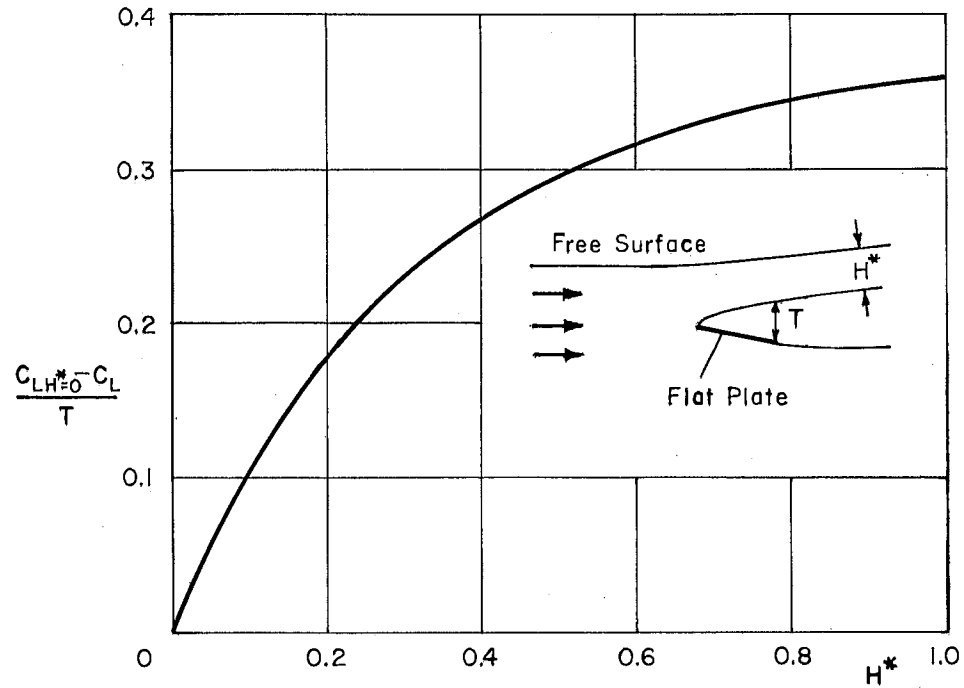


Fig. 15 - Relationship between Cavity Thickness T and the Change in Lift Coefficient as Related to Submergences H^* for the Flat Plate

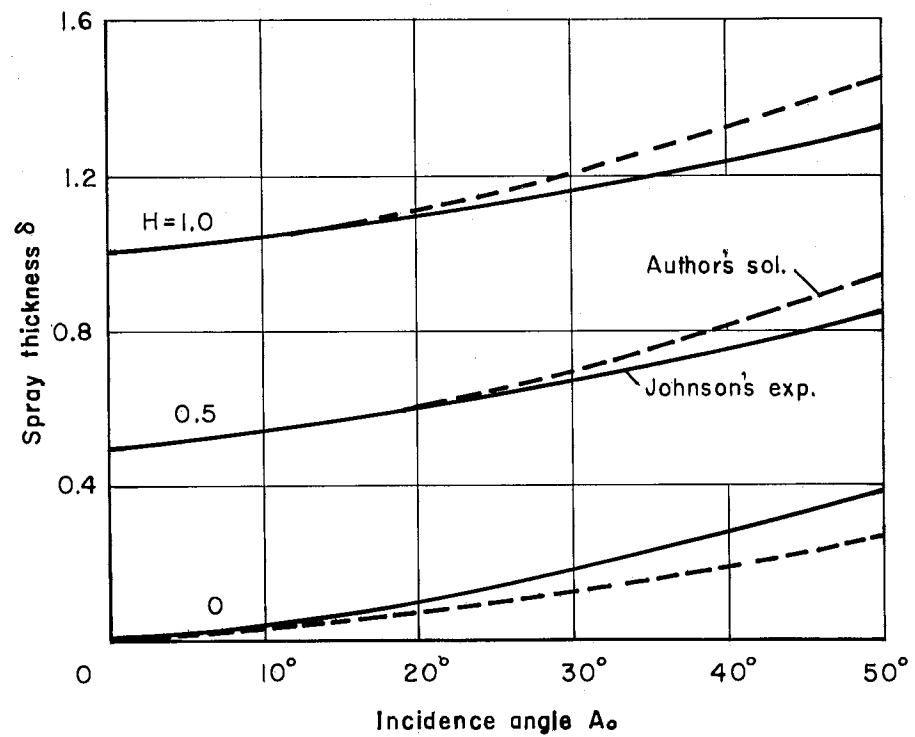


Fig. 16 - Comparison between the Calculated Spray Thickness δ and the Experimental One by Johnson

APPENDIX

APPENDIX

An attempt will be made to compare the solution presented in this paper with Green's exact solution [1] for flat plate hydrofoils operating at arbitrary submergences.

If the incidence angle A_0 is small of the first order $O(\epsilon)$,

$$\sin A_0 = A_0 + O(\epsilon^3), \quad \cos A_1 = 1 + O(\epsilon^2)$$

In the physical sense, Green's parameter b corresponding to the submergence H and/or the spray thickness δ , may be expressed by the parameter a as follows:

$$b = 1 + 2a$$

$$\therefore b - \sqrt{b^2 - 1} = 1 + 2a - 2a \sqrt{1 + \frac{1}{a}} = a_1$$

Green's force parameter K is

$$K = (b - \sqrt{b^2 - 1}) \sin A_0 + \frac{1}{\pi} [2 \cos A_0 + (b \cos A_0 - 1) \log \frac{b-1}{b+1}]$$

$$= a_1 A_0 + \frac{2}{\pi A} + O(\epsilon^2)$$

$$= \frac{2}{\pi A} \left(1 + \frac{C_L}{2}\right) + O(\epsilon^2) \quad (a)$$

$$\therefore \delta = \frac{1}{K} (b - \cos A_0) = H + \frac{1 - \cos A_0}{K} + O(\epsilon^2) \equiv H^* \quad (b)$$

Notice that $\frac{1 - \cos A_0}{K} \sim O(\epsilon)$, as $K \sim O(\epsilon)$. The H vs δ relation was estimated and is shown in Fig. 16 in parametric form in which Johnson's experimental values [5] are also referred to. Comparing the calculated values and the experimental ones, the accuracy of Eqs. (a) and (b) seems to be sufficiently good for practical incidence angles of $A_0 < 20^\circ$. If the incidence angle is quite small (for example, $A_0 < 5^\circ$), the value of $\frac{1 - \cos A_0}{K}$ may be

fairly small. Thus the assumption $H \approx H^*$ (see Refs. [2][3][5]) might be substantiated.

Since the disturbance in the free water level associated with the presence of the hydrofoil (and the spray angle) is related to the shape parameter A_0 (see Fig. 5), the H vs H^* relation for arbitrary shape hydrofoils might be estimated approximately by Eqs. (a) and (b) by picking up only the A_0 term.

Assuming that the modified submergence H^* of this paper is equal to the spray thickness δ , the lift and the drag coefficients C_L and C_D are

$$C_{L \text{ exact}} = \frac{2(b - \sqrt{b^2 - 1})}{K} \sin A_0 \cos A_0 = \frac{\pi a_1 A A_0 \cos A_0}{1 + \frac{C_L}{2}} + O(\epsilon^3)$$

$$= \frac{1}{J} C_{L \text{ linearized}} + O(\epsilon^3) = C_L + O(\epsilon^3)$$

$$C_{D \text{ exact}} = \frac{1}{J} C_{D \text{ linearized}} + O(\epsilon^3) = C_D + O(\epsilon^3)$$

where

$$J = \frac{1 + \frac{C_L}{2}}{\cos A_0} + O(\epsilon^2)$$

Therefore, if these linearized solutions are modified by a correction factor J as mentioned above, they agree with Green's exact solutions, up to second order terms.

SPONSOR'S DISTRIBUTION LIST FOR TECHNICAL PAPER 54-B
of the St. Anthony Falls Hydraulic Laboratory

<u>Copies</u>	<u>Organization</u>
6	Chief of Naval Research, Department of the Navy, Washington, D. C. 20360, Attn: 3 - Code 438 1 - Code 461 1 - Code 463 1 - Code 466
1	Commanding Officer, Office of Naval Research, Branch Office, 495 Summer Street, Boston 10, Massachusetts.
1	Commanding Officer, Office of Naval Research, Branch Office, 219 S. Dearborn St., Chicago, Illinois 60604.
1	Commanding Officer, Office of Naval Research, Branch Office, 207 West 24th Street, New York 11, New York.
25	Commanding Officer, Office of Naval Research, Branch Office, Navy No. 100, Box 39, Fleet Post Office, New York, New York.
1	Commanding Officer, Office of Naval Research, Branch Office, 1030 East Green Street, Pasadena 1, California.
1	Commanding Officer, Office of Naval Research, Branch Office, 1000 Geary Street, San Francisco 9, California.
6	Director, Naval Research Laboratory, Washington 25, D. C., Attn: Code 2027.
3	Chief, Bureau of Naval Weapons, Department of the Navy, Washington 25, D. C., Attn: 1 - Code RRRE 1 - Code RAAD 1 - Code RAAD-222
7	Chief, Bureau of Ships, Department of the Navy, Washington 25, D. C., Attn: 1 - Code 312 1 - Code 335 1 - Code 420 1 - Code 421 1 - Code 440 1 - Code 442 1 - Code 449
1	Chief, Bureau of Yards and Docks, Department of the Navy, Washington 25, D. C., Attn: Code D-400.
12	Commanding Officer and Director, David Taylor Model Basin, Washington 7, D. C., Attn: 1 - Code 500 1 - Code 513 1 - Code 520 1 - Code 525 1 - Code 526

CopiesOrganization

- 1 - Code 526A
 - 1 - Code 530
 - 1 - Code 533
 - 1 - Code 580
 - 1 - Code 585
 - 1 - Code 589
 - 1 - Code 700
-
- 1 Commander, Naval Ordnance Test Station, China Lake, California, Attn: Code 753.
 - 1 Commander, Naval Ordnance Test Station, Pasadena Annex, 3202 E. Foothill Boulevard, Pasadena 8, California, Attn: Code P508.
 - 1 Commander, Portsmouth Naval Shipyard, Portsmouth, New Hampshire, Attn: Planning Department.
 - 1 Commander, Boston Naval Shipyard, Boston, Massachusetts, Attn: Planning Department.
 - 1 Commander, Pearl Harbor Naval Shipyard, Navy No. 128, Fleet Post Office, San Francisco, California, Attn: Planning Department.
 - 1 Commander, San Francisco Naval Shipyard, San Francisco, California, Attn: Planning Department.
 - 1 Commander, Mare Island Naval Shipyard, Vallejo, California, Attn: Planning Department.
 - 1 Commander, New York Naval Shipyard, Brooklyn 1, New York, Attn: Planning Department.
 - 1 Commander, Puget Sound Naval Shipyard, Bremerton, Washington, Attn: Planning Department.
 - 1 Commander, Philadelphia Naval Shipyard, Philadelphia, Pennsylvania, Attn: Planning Department.
 - 1 Commander, Norfolk Naval Shipyard, Portsmouth, Virginia, Attn: Planning Department.
 - 1 Commander, Charleston Naval Shipyard, Charleston, South Carolina, Attn: Planning Department.
 - 1 Commander, Long Beach Naval Shipyard, Long Beach 2, California, Attn: Planning Department.
 - 1 Commander, US Naval Weapons Laboratory, Dahlgren, Virginia, Attn: Planning Department.
 - 1 Commander, US Naval Ordnance Laboratory, White Oak, Maryland.
 - 1 Commander, US Naval Weapons Laboratory, Dahlgren, Virginia, Attn: Computation and Exterior Ballistics Laboratory (Dr. A. V. Hershey).
 - 1 Superintendent, US Naval Academy, Annapolis, Maryland, Attn: Library.
 - 1 Superintendent, US Naval Postgraduate School, Monterey, California.
 - 1 Commandant, US Coast Guard, 1300 E Street NW, Washington, D. C.
 - 1 Secretary, Ship Structure Committee, US Coast Guard Headquarters, 1300 E Street NW, Washington, D. C.

CopiesOrganization

- 1 Commander, Military Sea Transportation Service, Department of the Navy, Washington 25, D. C.
- 1 Division of Ship Design, Maritime Administration, 441 G Street NW, Washington 25, D. C.
- 1 Superintendent, US Merchant Marine Academy, Kings Point, Long Island, New York, Attn: Captain L. S. McCready.
- 1 Commanding Officer and Director, US Navy Mine Defense Laboratory, Panama City, Florida.
- 1 Commanding Officer, NROTC and Naval Administrative Unit, Massachusetts Institute of Technology, Cambridge 39, Massachusetts.
- 1 Commander, Hdqs. US Army Transportation Research and Development Command, Transportation Corps, Fort Eustis, Virginia, Attn: Marine Transportation Division.
- 1 Air Force Office of Scientific Research, Mechanics Division, Washington 25, D. C.
- 1 Commander, Wright Air Development Division, Aircraft Laboratory, Wright-Patterson Air Force Base, Ohio, Attn: Mr. W. Mykytow, Dynamics Branch.
- 1 Director of Research, Code RR, National Aeronautics and Space Administration, 600 Independence Avenue SW, Washington, D. C. 20546.
- 1 Director, Langley Research Center, Langley Station, Hampton, Virginia, Attn: Mr. I. E. Garrick.
- 1 Director, Langley Research Center, Langley Station, Hampton, Virginia, Attn: Mr. D. J. Marten.
- 1 Director, Engineering Science Division, National Science Foundation, Washington, D. C.
- 1 Director, National Bureau of Standards, Washington 25, D. C., Attn: Mr. J. M. Franklin.
- 1 Dr. G. B. Schubauer, Fluid Mechanics Section, National Bureau of Standards, Washington 25, D. C.
- 20 Defense Documentation Center, Cameron Station, Alexandria, Virginia.
- 1 Clearinghouse, 5285 Port Royal Road, Springfield, Virginia 22151.
- 1 Mr. Alfonso Alcadan L., Director, Laboratorio Nacional de Hidraulica, Antiguo Camino A Ancon, Casilla Postal 682, Lima, Peru.
- 1 Mr. T. A. Duncan, Lycoming Division, AVCO Corporation, 1701 K Street NW, Apartment 904, Washington, D. C.
- 1 Baker Manufacturing Company, Evansville, Wisconsin.
- 1 Professor S. Siestrunk, Bureau D'Analyse et de Recherche Appliquees, 47, Avenue Victor Cresson, Issy-Les-Moulineaux, Seine, France.
- 1 Professor A. Acosta, California Institute of Technology, Pasadena 4, California.

CopiesOrganization

- 1 Professor M. Plesset, California Institute of Technology, Pasadena 4, California.
- 1 Professor T. Y. Wu, California Institute of Technology, Pasadena 4, California.
- 1 Professor A. Powell, University of California, Los Angeles, California.
- 1 Dr. Maurice L. Albertson, Professor of Civil Engineering, Colorado State University, Fort Collins, Colorado 80521.
- 1 Professor J. E. Cermak, Colorado State University, Department of Civil Engineering, Fort Collins, Colorado.
- 1 Dr. Blaine R. Parkin, General Dynamics - Convair, P. O. Box 1950, San Diego 12, California.
- 1 Mr. Robert H. Oversmith, Chief of ASW/Marine Sciences, Mail Zone 6-107, General Dynamics - Convair, San Diego, California 92112.
- 1 Dr. Irving C. Statler, Head, Applied Mechanics Department, Cornell Aeronautical Laboratory, Inc., P. O. Box 235, Buffalo, New York 14221.
- 1 Mr. Richard P. White, Jr., Cornell Aeronautical Laboratory, 4455 Genesee Street, Buffalo, New York.
- 1 Professor W. R. Sears, Graduate School of Aeronautical Engineering, Cornell University, Ithaca, New York.
- 1 Mr. George H. Pedersen, Curtiss-Wright Corporation, Wright Aeronautical Division, Wood-Ridge, New Jersey, Location CC-1 Engrg. Mezz.
- 1 Mr. G. Tedrew, Food Machinery Corporation, P. O. Box 367, San Jose, California.
- 1 General Applied Science Laboratory, Merrick and Stewart Avenues, Westbury, Long Island, New York, Attn: Dr. Frank Lane.
- 1 Mr. R. McCandliss, Electric Boat Division, General Dynamics Corporation, Groton, Connecticut.
- 1 Dr. A. S. Iberall, President, General Technical Services, Inc., 2640 Whiton Road, Cleveland 18, Ohio.
- 1 Gibbs and Cox, Inc., 21 West Street, New York, New York 10006.
- 1 Mr. Eugene F. Baird, Chief of Dynamic Analysis, Grumman Aircraft Engineering Corporation, Bethpage, Long Island, New York.
- 1 Mr. Robert E. Bower, Chief, Advanced Development, Grumman Aircraft Engineering Corporation, Bethpage, Long Island, New York.
- 1 Mr. William P. Carl, Grumman Aircraft Engineering Corporation, Bethpage, Long Island, New York.
- 1 Grumman Aircraft Engineering Corporation, Research Department, Plant 25, Bethpage, Long Island, New York 11714, Attn: Mr. Kenneth Keen.
- 1 Dr. O. Grim, Hamburgische Schiffbau-Versuchsanstalt, Bramfelder Strasse 164, Hamburg 33, Germany.

CopiesOrganization

- 1 Dr. H. W. Lerbs, Hamburgische Schiffbau-Versuchsanstalt, Bramfelder Strasse 164, Hamburg 33, Germany.
- 1 Dr. H. Schwanecke, Hamburgische Schiffbau-Versuchsanstalt, Bramfelder Strasse 164, Hamburg 33, Germany.
- 1 Professor G. P. Weinblum, Director, Institute for Schiffbau, University of Hamburg, Berliner Tow 21, Hamburg, Germany.
- 1 Professor G. F. Carrier, Harvard University, Cambridge 38, Massachusetts.
- 1 Dr. S. F. Hoerner, 148 Busted Drive, Midland Park, New Jersey.
- 1 Mr. P. Eisenberg, President, Hydronautics, Incorporated, Pindell School Road, Howard County, Laurel, Maryland.
- 1 Professor Carl Prohaska, Hydro-og Aerodynamisk Laboratorium, Lyngby, Denmark.
- 1 Professor L. Landweber, Iowa Institute of Hydraulic Research, State University of Iowa, Iowa City, Iowa.
- 1 Professor H. Rouse, Iowa Institute of Hydraulic Research, State University of Iowa, Iowa City, Iowa.
- 1 Professor S. Corrsin, Department of Mechanics, The Johns Hopkins University, Baltimore 18, Maryland.
- 2 Professor O. M. Phillips, Division of Mechanical Engineering, Institute for Cooperative Research, The Johns Hopkins University, Baltimore 18, Maryland.
- 1 Mr. Bill East, Lockheed Aircraft Corporation, California Division, Hydrodynamics Research, Burbank, California.
- 1 Mr. R. W. Kermeen, Lockheed Missiles and Space Company, Department 81-73/Bldg 538, P. O. Box 504, Sunnyvale, California.
- 1 Department of Naval Architecture and Marine Engineering, Room 5-228, Massachusetts Institute of Technology, 77 Massachusetts Avenue, Cambridge, Massachusetts 02139.
- 1 Professor M. A. Abkowitz, Massachusetts Institute of Technology, Cambridge 39, Massachusetts.
- 1 Professor H. Ashley, Massachusetts Institute of Technology, Cambridge 39, Massachusetts.
- 1 Professor A. T. Ippen, Massachusetts Institute of Technology, Cambridge 39, Massachusetts.
- 1 Professor M. Landahl, Massachusetts Institute of Technology, Cambridge 39, Massachusetts.
- 1 Dr. H. Reichardt, Director, Max-Planck Institut fur Stromungsfor- schung, Bottingerstrasse 6-8, Gottingen, Germany.
- 1 Professor R. B. Couch, University of Michigan, Ann Arbor, Michigan.
- 1 Professor W. W. Willmarth, University of Michigan, Ann Arbor, Michigan.

<u>Copies</u>	<u>Organization</u>
1	Midwest Research Institute, 425 Volker Boulevard, Kansas City, Missouri, Attn: Library.
1	Director, St. Anthony Falls Hydraulic Laboratory, University of Minnesota, Minneapolis 14, Minnesota.
1	Dr. C. S. Song, St. Anthony Falls Hydraulic Laboratory, University of Minnesota, Minneapolis 14, Minnesota.
1	Mr. J. M. Wetzel, St. Anthony Falls Hydraulic Laboratory, University of Minnesota, Minneapolis 14, Minnesota.
1	Head, Aerodynamics Division, National Physical Laboratory, Teddington, Middlesex, England.
1	Mr. A. Silverleaf, National Physical Laboratory, Teddington, Middlesex, England.
1	The Aeronautical Library, National Research Council, Montreal Road, Ottawa 2, Canada.
1	Dr. J. B. Van Manen, Netherlands Ship Model Basin, Wageningen, The Netherlands.
1	Professor John J. Foody, Chairman, Engineering Department, State University of New York, Maritime College, Bronx, New York 10465.
1	Professor J. Keller, Institute of Mathematical Sciences, New York University, 25 Waverly Place, New York 3, New York.
1	Professor J. J. Stoker, Institute of Mathematical Sciences, New York University, 25 Waverly Place, New York 3, New York.
1	Dr. T. R. Goodman, Oceanics, Incorporated, Technical Industrial Park, Plainview, Long Island, New York.
1	Professor J. William Holl, Department of Aeronautical Engineering, The Pennsylvania State University, Ordnance Research Laboratory, P. O. Box 30, University Park, Pennsylvania.
1	Dr. M. Sevik, Ordnance Research Laboratory, Pennsylvania State University, University Park, Pennsylvania.
1	Dr. George F. Wislicenus, Garfield Thomas Water Tunnel, Ordnance Research Laboratory, The Pennsylvania State University, Post Office Box 30, University Park, Pennsylvania 16801.
1	Mr. David Wellinger, Hydrofoil Projects, Radio Corporation of America, Burlington, Massachusetts.
1	The RAND Corporation, 1700 Main Street, Santa Monica, California 90406, Attn: Library.
1	Professor R. C. DiPrima, Department of Mathematics, Rensselaer Polytechnic Institute, Troy, New York.
1	Mr. L. M. White, U. S. Rubber Company, Research and Development Department, Wayne, New Jersey.
1	Professor J. K. Lunde, Skipsmodelltanken, Trondheim, Norway.
1	Editor, Applied Mechanics Review, Southwest Research Institute, 8500 Culebra Road, San Antonio 6, Texas.

CopiesOrganization

- 1 Dr. H. N. Abramson, Southwest Research Institute, 8500 Culebra Road, San Antonio 6, Texas.
- 1 Mr. G. Ransleben, Southwest Research Institute, 8500 Culebra Road, San Antonio 6, Texas.
- 1 Professor E. Y. Hsu, Stanford University, Stanford, California.
- 1 Dr. Byrne Perry, Department of Civil Engineering, Stanford University, Stanford, California 94305.
- 1 Dr. J. P. Breslin, Stevens Institute of Technology, Davidson Laboratory, Hoboken, New Jersey.
- 1 Mr. D. Savitsky, Stevens Institute of Technology, Davidson Laboratory, Hoboken, New Jersey.
- 1 Mr. S. Tsakonas, Stevens Institute of Technology, Davidson Laboratory, Hoboken, New Jersey.
- 1 Dr. Jack Kotik, Technical Research Group, Inc., Route 110, Melville, New York.
- 1 Dr. R. Timman, Department of Applied Mathematics, Technological University, Julianalaan 132, Delft, Holland.
- 1 The Transportation Technical Research Institute, Investigation Office, Ship Research Institute, 700 Shinkawa, Mitaka, Tokyo-to, Japan.
- 1 Dr. Grosse, Versuchsanstalt fur Wasserbau und Schiffbau, Schleuseninsel im Tiergarten, Berlin, Germany.
- 1 Dr. S. Schuster, Director, Versuchsanstalt fur Wasserbau und Schiffbau, Schleuseninsel im Tiergarten, Berlin, Germany.
- 1 Technical Library, Webb Institute of Naval Architecture, Glen Cove, Long Island, New York.
- 1 Professor E. V. Lewis, Webb Institute of Naval Architecture, Glen Cove, Long Island, New York.
- 1 Mr. C. Wigley, Flat 103, 6-9 Charterhouse Square, London E. C. 1, England.
- 1 Coordinator of Research, Maritime Administration, 441 G Street NW, Washington 25, D. C.

Unclassified

Security Classification

DOCUMENT CONTROL DATA - R&D

(Security classification of title, body of abstract and indexing annotation must be entered when the overall report is classified)

1. ORIGINATING ACTIVITY (Corporate author) St. Anthony Falls Hydraulic Laboratory, University of Minnesota		2 a. REPORT SECURITY CLASSIFICATION Unclassified	
		2 b. GROUP	
3. REPORT TITLE ON THE EXISTENCE OF ZERO FORM-DRAG AND HYDRODYNAMICALLY STABLE SUPERCAVITATING HYDROFOILS			
4. DESCRIPTIVE NOTES (Type of report and inclusive dates) Final report on this aspect of study			
5. AUTHOR(S) (Last name, first name, initial) Oba, R.			
6. REPORT DATE November 1965		7 a. TOTAL NO. OF PAGES 46	7 b. NO. OF REFS 14
8 a. CONTRACT OR GRANT NO. Nonr 710(24)		9 a. ORIGINATOR'S REPORT NUMBER(S) Technical Paper No. 54-B	
b. PROJECT NO. NR 062-052		9 b. OTHER REPORT NO(S) (Any other numbers that may be assigned this report)	
c.			
d.			
10. AVAILABILITY/LIMITATION NOTICES Qualified requestors may obtain copies of this report from DDC.			
11. SUPPLEMENTARY NOTES		12. SPONSORING MILITARY ACTIVITY Office of Naval Research	
13. ABSTRACT The linearized complex acceleration potential is obtained for a hydrofoil of arbitrary shape in steady motion beneath a free surface with cavity of infinite length in simple and compact form. Using some numerical results obtained from the complex potential, it is shown that there exists theoretically a supercavitating hydrofoil with finite lift coefficient and zero form drag. It is also shown that there exists theoretically a supercavitating hydrofoil with stable characteristics when shallowly submerged; that is, the lift coefficient increases as the submergence increases.			

14. KEY WORDS	LINK A		LINK B		LINK C	
	ROLE	WT	ROLE	WT	ROLE	WT
Supercavitating Hydrofoil Drag Reduction Stability						

INSTRUCTIONS

1. **ORIGINATING ACTIVITY:** Enter the name and address of the contractor, subcontractor, grantee, Department of Defense activity or other organization (*corporate author*) issuing the report.
- 2a. **REPORT SECURITY CLASSIFICATION:** Enter the overall security classification of the report. Indicate whether "Restricted Data" is included. Marking is to be in accordance with appropriate security regulations.
- 2b. **GROUP:** Automatic downgrading is specified in DoD Directive 5200.10 and Armed Forces Industrial Manual. Enter the group number. Also, when applicable, show that optional markings have been used for Group 3 and Group 4 as authorized.
3. **REPORT TITLE:** Enter the complete report title in all capital letters. Titles in all cases should be unclassified. If a meaningful title cannot be selected without classification, show title classification in all capitals in parenthesis immediately following the title.
4. **DESCRIPTIVE NOTES:** If appropriate, enter the type of report, e.g., interim, progress, summary, annual, or final. Give the inclusive dates when a specific reporting period is covered.
5. **AUTHOR(S):** Enter the name(s) of author(s) as shown on or in the report. Enter last name, first name, middle initial. If military, show rank and branch of service. The name of the principal author is an absolute minimum requirement.
6. **REPORT DATE:** Enter the date of the report as day, month, year; or month, year. If more than one date appears on the report, use date of publication.
- 7a. **TOTAL NUMBER OF PAGES:** The total page count should follow normal pagination procedures, i.e., enter the number of pages containing information.
- 7b. **NUMBER OF REFERENCES:** Enter the total number of references cited in the report.
- 8a. **CONTRACT OR GRANT NUMBER:** If appropriate, enter the applicable number of the contract or grant under which the report was written.
- 8b, 8c, & 8d. **PROJECT NUMBER:** Enter the appropriate military department identification, such as project number, subproject number, system numbers, task number, etc.
- 9a. **ORIGINATOR'S REPORT NUMBER(S):** Enter the official report number by which the document will be identified and controlled by the originating activity. This number must be unique to this report.
- 9b. **OTHER REPORT NUMBER(S):** If the report has been assigned any other report numbers (*either by the originator or by the sponsor*), also enter this number(s).
10. **AVAILABILITY/LIMITATION NOTICES:** Enter any limitations on further dissemination of the report, other than those

imposed by security classification, using standard statements such as:

- (1) "Qualified requesters may obtain copies of this report from DDC."
- (2) "Foreign announcement and dissemination of this report by DDC is not authorized."
- (3) "U. S. Government agencies may obtain copies of this report directly from DDC. Other qualified DDC users shall request through _____."
- (4) "U. S. military agencies may obtain copies of this report directly from DDC. Other qualified users shall request through _____."
- (5) "All distribution of this report is controlled. Qualified DDC users shall request through _____."

If the report has been furnished to the Office of Technical Services, Department of Commerce, for sale to the public, indicate this fact and enter the price, if known.

11. **SUPPLEMENTARY NOTES:** Use for additional explanatory notes.
12. **SPONSORING MILITARY ACTIVITY:** Enter the name of the departmental project office or laboratory sponsoring (*paying for*) the research and development. Include address.
13. **ABSTRACT:** Enter an abstract giving a brief and factual summary of the document indicative of the report, even though it may also appear elsewhere in the body of the technical report. If additional space is required, a continuation sheet shall be attached.

It is highly desirable that the abstract of classified reports be unclassified. Each paragraph of the abstract shall end with an indication of the military security classification of the information in the paragraph, represented as (TS), (S), (C), or (U).

There is no limitation on the length of the abstract. However, the suggested length is from 150 to 225 words.

14. **KEY WORDS:** Key words are technically meaningful terms or short phrases that characterize a report and may be used as index entries for cataloging the report. Key words must be selected so that no security classification is required. Identifiers, such as equipment model designation, trade name, military project code name, geographic location, may be used as key words but will be followed by an indication of technical context. The assignment of links, roles, and weights is optional.

Technical Paper No. 54, Series B
St. Anthony Falls Hydraulic Laboratory

ON THE EXISTENCE OF ZERO FORM-DRAG AND HYDRODYNAMICALLY STABLE SUPERCAVITATING HYDROFOILS, by R. Ōba. November 1965. 46 pages incl. 16 illus. Contract Nonr 710(24).

The linearized complex acceleration potential is obtained for a hydrofoil of arbitrary shape in steady motion beneath a free surface with cavity of infinite length in simple and compact form. Using some numerical results obtained from the complex potential, it is shown that there exists theoretically a supercavitating hydrofoil with stable characteristics when shallowly submerged; that is, the lift coefficient increases as the submergence increases.

Available from St. Anthony Falls Hydraulic Laboratory, University of Minnesota, at \$1.50 per copy.

1. Supercavitating Flow
 2. Hydrofoil
 3. Drag Reduction
 4. Zero Drag
 5. Stability
 6. Acceleration Potential
 7. Linear Theory
- I. Title
II. Ōba, R.
III. St. Anthony Falls Hydraulic Laboratory
IV. Contract No. Nonr 710(24)

Unclassified

Technical Paper No. 54, Series B
St. Anthony Falls Hydraulic Laboratory

ON THE EXISTENCE OF ZERO FORM-DRAG AND HYDRODYNAMICALLY STABLE SUPERCAVITATING HYDROFOILS, by R. Ōba. November 1965. 46 pages incl. 16 illus. Contract Nonr 710(24).

The linearized complex acceleration potential is obtained for a hydrofoil of arbitrary shape in steady motion beneath a free surface with cavity of infinite length in simple and compact form. Using some numerical results obtained from the complex potential, it is shown that there exists theoretically a supercavitating hydrofoil with stable characteristics when shallowly submerged; that is, the lift coefficient increases as the submergence increases.

Available from St. Anthony Falls Hydraulic Laboratory, University of Minnesota, at \$1.50 per copy.

1. Supercavitating Flow
 2. Hydrofoil
 3. Drag Reduction
 4. Zero Drag
 5. Stability
 6. Acceleration Potential
 7. Linear Theory
- I. Title
II. Ōba, R.
III. St. Anthony Falls Hydraulic Laboratory
IV. Contract No. Nonr 710(24)

Unclassified

Technical Paper No. 54, Series B
St. Anthony Falls Hydraulic Laboratory

ON THE EXISTENCE OF ZERO FORM-DRAG AND HYDRODYNAMICALLY STABLE SUPERCAVITATING HYDROFOILS, by R. Ōba. November 1965. 46 pages incl. 16 illus. Contract Nonr 710(24).

The linearized complex acceleration potential is obtained for a hydrofoil of arbitrary shape in steady motion beneath a free surface with cavity of infinite length in simple and compact form. Using some numerical results obtained from the complex potential, it is shown that there exists theoretically a supercavitating hydrofoil with stable characteristics when shallowly submerged; that is, the lift coefficient increases as the submergence increases.

Available from St. Anthony Falls Hydraulic Laboratory, University of Minnesota, at \$1.50 per copy.

1. Supercavitating Flow
 2. Hydrofoil
 3. Drag Reduction
 4. Zero Drag
 5. Stability
 6. Acceleration Potential
 7. Linear Theory
- I. Title
II. Ōba, R.
III. St. Anthony Falls Hydraulic Laboratory
IV. Contract No. Nonr 710(24)

Unclassified

Technical Paper No. 54, Series B
St. Anthony Falls Hydraulic Laboratory

ON THE EXISTENCE OF ZERO FORM-DRAG AND HYDRODYNAMICALLY STABLE SUPERCAVITATING HYDROFOILS, by R. Ōba. November 1965. 46 pages incl. 16 illus. Contract Nonr 710(24).

The linearized complex acceleration potential is obtained for a hydrofoil of arbitrary shape in steady motion beneath a free surface with cavity of infinite length in simple and compact form. Using some numerical results obtained from the complex potential, it is shown that there exists theoretically a supercavitating hydrofoil with stable characteristics when shallowly submerged; that is, the lift coefficient increases as the submergence increases.

Available from St. Anthony Falls Hydraulic Laboratory, University of Minnesota, at \$1.50 per copy.

1. Supercavitating Flow
 2. Hydrofoil
 3. Drag Reduction
 4. Zero Drag
 5. Stability
 6. Acceleration Potential
 7. Linear Theory
- I. Title
II. Ōba, R.
III. St. Anthony Falls Hydraulic Laboratory
IV. Contract No. Nonr 710(24)

Unclassified

Technical Paper No. 54, Series B
St. Anthony Falls Hydraulic Laboratory

ON THE EXISTENCE OF ZERO FORM-DRAG AND HYDRODYNAMICALLY STABLE SUPERCAVITATING HYDROFOILS, by R. Ōba. November 1965. 46 pages incl. 16 illus. Contract Nonr 710(24).

The linearized complex acceleration potential is obtained for a hydrofoil of arbitrary shape in steady motion beneath a free surface with cavity of infinite length in simple and compact form. Using some numerical results obtained from the complex potential, it is shown that there exists theoretically a supercavitating hydrofoil with stable characteristics when shallowly submerged; that is, the lift coefficient increases as the submergence increases.

Available from St. Anthony Falls Hydraulic Laboratory, University of Minnesota, at \$1.50 per copy.

1. Supercavitating Flow
2. Hydrofoil
3. Drag Reduction
4. Zero Drag
5. Stability
6. Acceleration Potential
7. Linear Theory

- I. Title
- II. Ōba, R.
- III. St. Anthony Falls Hydraulic Laboratory
- IV. Contract No. Nonr 710(24)

Unclassified

Technical Paper No. 54, Series B
St. Anthony Falls Hydraulic Laboratory

ON THE EXISTENCE OF ZERO FORM-DRAG AND HYDRODYNAMICALLY STABLE SUPERCAVITATING HYDROFOILS, by R. Ōba. November 1965. 46 pages incl. 16 illus. Contract Nonr 710(24).

The linearized complex acceleration potential is obtained for a hydrofoil of arbitrary shape in steady motion beneath a free surface with cavity of infinite length in simple and compact form. Using some numerical results obtained from the complex potential, it is shown that there exists theoretically a supercavitating hydrofoil with stable characteristics when shallowly submerged; that is, the lift coefficient increases as the submergence increases.

Available from St. Anthony Falls Hydraulic Laboratory, University of Minnesota, at \$1.50 per copy.

1. Supercavitating Flow
2. Hydrofoil
3. Drag Reduction
4. Zero Drag
5. Stability
6. Acceleration Potential
7. Linear Theory

- I. Title
- II. Ōba, R.
- III. St. Anthony Falls Hydraulic Laboratory
- IV. Contract No. Nonr 710(24)

Unclassified

Technical Paper No. 54, Series B
St. Anthony Falls Hydraulic Laboratory

ON THE EXISTENCE OF ZERO FORM-DRAG AND HYDRODYNAMICALLY STABLE SUPERCAVITATING HYDROFOILS, by R. Ōba. November 1965. 46 pages incl. 16 illus. Contract Nonr 710(24).

The linearized complex acceleration potential is obtained for a hydrofoil of arbitrary shape in steady motion beneath a free surface with cavity of infinite length in simple and compact form. Using some numerical results obtained from the complex potential, it is shown that there exists theoretically a supercavitating hydrofoil with stable characteristics when shallowly submerged; that is, the lift coefficient increases as the submergence increases.

Available from St. Anthony Falls Hydraulic Laboratory, University of Minnesota, at \$1.50 per copy.

1. Supercavitating Flow
2. Hydrofoil
3. Drag Reduction
4. Zero Drag
5. Stability
6. Acceleration Potential
7. Linear Theory

- I. Title
- II. Ōba, R.
- III. St. Anthony Falls Hydraulic Laboratory
- IV. Contract No. Nonr 710(24)

Unclassified

Technical Paper No. 54, Series B
St. Anthony Falls Hydraulic Laboratory

ON THE EXISTENCE OF ZERO FORM-DRAG AND HYDRODYNAMICALLY STABLE SUPERCAVITATING HYDROFOILS, by R. Ōba. November 1965. 46 pages incl. 16 illus. Contract Nonr 710(24).

The linearized complex acceleration potential is obtained for a hydrofoil of arbitrary shape in steady motion beneath a free surface with cavity of infinite length in simple and compact form. Using some numerical results obtained from the complex potential, it is shown that there exists theoretically a supercavitating hydrofoil with stable characteristics when shallowly submerged; that is, the lift coefficient increases as the submergence increases.

Available from St. Anthony Falls Hydraulic Laboratory, University of Minnesota, at \$1.50 per copy.

1. Supercavitating Flow
2. Hydrofoil
3. Drag Reduction
4. Zero Drag
5. Stability
6. Acceleration Potential
7. Linear Theory

- I. Title
- II. Ōba, R.
- III. St. Anthony Falls Hydraulic Laboratory
- IV. Contract No. Nonr 710(24)

Unclassified

Technical Paper No. 54, Series B
St. Anthony Falls Hydraulic Laboratory

ON THE EXISTENCE OF ZERO FORM-DRAG AND HYDRODYNAMICALLY STABLE SUPERCAVITATING HYDROFOILS, by R. Ōba. November 1965. 46 pages incl. 16 illus. Contract Nonr 710(24).

The linearized complex acceleration potential is obtained for a hydrofoil of arbitrary shape in steady motion beneath a free surface with cavity of infinite length in simple and compact form. Using some numerical results obtained from the complex potential, it is shown that there exists theoretically a supercavitating hydrofoil with stable characteristics when shallowly submerged; that is, the lift coefficient increases as the submergence increases.

Available from St. Anthony Falls Hydraulic Laboratory, University of Minnesota, at \$1.50 per copy.

1. Supercavitating Flow
2. Hydrofoil
3. Drag Reduction
4. Zero Drag
5. Stability
6. Acceleration Potential
7. Linear Theory

- I. Title
- II. Ōba, R.
- III. St. Anthony Falls Hydraulic Laboratory
- IV. Contract No. Nonr 710(24)

Unclassified

Technical Paper No. 54, Series B
St. Anthony Falls Hydraulic Laboratory

ON THE EXISTENCE OF ZERO FORM-DRAG AND HYDRODYNAMICALLY STABLE SUPERCAVITATING HYDROFOILS, by R. Ōba. November 1965. 46 pages incl. 16 illus. Contract Nonr 710(24).

The linearized complex acceleration potential is obtained for a hydrofoil of arbitrary shape in steady motion beneath a free surface with cavity of infinite length in simple and compact form. Using some numerical results obtained from the complex potential, it is shown that there exists theoretically a supercavitating hydrofoil with stable characteristics when shallowly submerged; that is, the lift coefficient increases as the submergence increases.

Available from St. Anthony Falls Hydraulic Laboratory, University of Minnesota, at \$1.50 per copy.

1. Supercavitating Flow
2. Hydrofoil
3. Drag Reduction
4. Zero Drag
5. Stability
6. Acceleration Potential
7. Linear Theory

- I. Title
- II. Ōba, R.
- III. St. Anthony Falls Hydraulic Laboratory
- IV. Contract No. Nonr 710(24)

Unclassified

Technical Paper No. 54, Series B
St. Anthony Falls Hydraulic Laboratory

ON THE EXISTENCE OF ZERO FORM-DRAG AND HYDRODYNAMICALLY STABLE SUPERCAVITATING HYDROFOILS, by R. Ōba. November 1965. 46 pages incl. 16 illus. Contract Nonr 710(24).

The linearized complex acceleration potential is obtained for a hydrofoil of arbitrary shape in steady motion beneath a free surface with cavity of infinite length in simple and compact form. Using some numerical results obtained from the complex potential, it is shown that there exists theoretically a supercavitating hydrofoil with stable characteristics when shallowly submerged; that is, the lift coefficient increases as the submergence increases.

Available from St. Anthony Falls Hydraulic Laboratory, University of Minnesota, at \$1.50 per copy.

1. Supercavitating Flow
2. Hydrofoil
3. Drag Reduction
4. Zero Drag
5. Stability
6. Acceleration Potential
7. Linear Theory

- I. Title
- II. Ōba, R.
- III. St. Anthony Falls Hydraulic Laboratory
- IV. Contract No. Nonr 710(24)

Unclassified

Technical Paper No. 54, Series B
St. Anthony Falls Hydraulic Laboratory

ON THE EXISTENCE OF ZERO FORM-DRAG AND HYDRODYNAMICALLY STABLE SUPERCAVITATING HYDROFOILS, by R. Ōba. November 1965. 46 pages incl. 16 illus. Contract Nonr 710(24).

The linearized complex acceleration potential is obtained for a hydrofoil of arbitrary shape in steady motion beneath a free surface with cavity of infinite length in simple and compact form. Using some numerical results obtained from the complex potential, it is shown that there exists theoretically a supercavitating hydrofoil with stable characteristics when shallowly submerged; that is, the lift coefficient increases as the submergence increases.

Available from St. Anthony Falls Hydraulic Laboratory, University of Minnesota, at \$1.50 per copy.

1. Supercavitating Flow
2. Hydrofoil
3. Drag Reduction
4. Zero Drag
5. Stability
6. Acceleration Potential
7. Linear Theory

- I. Title
- II. Ōba, R.
- III. St. Anthony Falls Hydraulic Laboratory
- IV. Contract No. Nonr 710(24)

Unclassified